

Novel and Updated Bounds on Flavor-violating Z Interactions in the Lepton Sector

Fayez Abu-Ajamieh ^{1,*}, Amine Ahriche ^{2,†} and Nobuchika Okada ^{3,‡}

¹*Center for High Energy Physics; Indian Institute of Science; Bangalore; India*

²*Department of Applied Physics and Astronomy; University of Sharjah; P.O. Box 27272 Sharjah; UAE*

³*Department of Physics and Astronomy; University of Alabama; Tuscaloosa; Alabama 35487; USA*

We investigate the experimental bounds on the Flavor-Violating (FV) couplings of the Z boson to the charged leptons. In addition to the direct LHC searches for FV Z decays to leptons, we investigate indirect bounds from flavor-conserving Z decays to leptons at 1-loop, bounds from LEP searches, Electroweak Precision Observables (EWPO), $\ell_i \rightarrow \ell_j \gamma$ decays, $\ell_i \rightarrow 3\ell_j$ decays, $\ell_i \rightarrow \ell_j + \text{inv.}$ decays, FV meson decays to leptons, FV τ decays to $\mu(e) + \text{mesons}$, muon conversion in nuclei, and from muonium-antimuonium oscillations. For FV Z couplings to $\tau\mu$, we find that $\tau \rightarrow \mu\gamma$ yields the strongest bounds, with a level reaching $\mathcal{O}(10^{-5})$, followed by bounds from $\tau \rightarrow 3\mu(\mu ee)$. For FV Z couplings to τe , we find that the strongest bounds arise from the decay $\tau \rightarrow \mu\mu e$, reaching $\mathcal{O}(10^{-7})$ as well, with bounds from $\tau \rightarrow 3e$ also yielding strong bounds. For FV Z couplings to μe , we find that the strongest bounds are obtained from the decay $\mu \rightarrow 3e$, reaching $\mathcal{O}(10^{-11})$, with bounds from $\mu \rightarrow e\gamma$, muon conversion, $K_L^0 \rightarrow \mu e$ and $\mu \rightarrow e + \text{inv.}$ also providing strong bounds. We also study projections from future experiments, such as the FCC-ee, Belle II and the Mu2e experiment. For the Z couplings to $\tau\mu$, we find that future experiments could improve the bound to $\mathcal{O}(10^{-6})$, whereas for the Z couplings to τe , we find that future experiments could improve the bound to $\mathcal{O}(10^{-8})$, and for the Z couplings to μe , they could improve the bound to $\mathcal{O}(10^{-13})$.

*Electronic address: fayezaajamieh@iisc.ac.in

†Electronic address: ahriche@sharjah.ac.ae

‡Electronic address: okadan@ua.edu

I. INTRODUCTION

The discovery of the Higgs boson at the Large Hadron Collider (LHC) marked a significant milestone in particle physics [1], completing the Standard Model (SM) framework. Despite this achievement, the SM falls short of addressing several fundamental questions, such as the origin of neutrino masses, the matter-antimatter asymmetry in the Universe, the nature of dark matter and dark energy, and the strong CP problem. These unresolved issues strongly suggest that the SM is not the ultimate theory but rather an Effective Field Theory (EFT) valid up to a certain Ultraviolet (UV) energy scale Λ . At this scale, New Physics (NP) phenomena are expected to emerge, manifesting as small deviations from the SM predictions that are suppressed by powers of Λ [2–5]. This perspective has motivated extensive efforts to explore BSM physics through both theoretical models and experimental searches.

There have been significant efforts to search for physics Beyond the Standard Model (BSM), with many proposals put forward. One such proposal involves searching for Flavor Violation (FV). It is known that the SM lacks any Flavor-Changing Neutral Currents (FCNC) [6]. The QED photon couples universally to charged fermions, depending only on their electric charge. In the SM Higgs sector, the Yukawa couplings do not violate flavor, and the SM Z boson also preserves flavor. However, incorporating FCNC in BSM physics is relatively straightforward with some minor assumptions.

FV in the Higgs sector has attracted significant attention over the years (see, for instance, [7–30]). As pointed out in [31], it is well known that in the SM, there exists an approximate $U(1)^5$ symmetry of light quarks, which is broken by the Yukawa couplings. Thus, UV interactions with the Higgs need not necessarily preserve flavor. However, the fact that FV at $\Lambda \sim$ a few TeV is experimentally excluded led the authors to propose the Minimal Flavor Violation (MFV) framework, in which all flavor- and CP-violating interactions are linked to known Yukawa interactions.

On the other hand, less attention has been given to studying FV in the Z sector [32–36] or the Z' sector [37–41]. In this work, we aim to update the bounds on FV Z interactions with charged leptons and establish novel constraints that, to the best of our knowledge, have not been previously calculated. We review the bounds arising from direct searches at the LHC for $Z \rightarrow \ell_i \ell_j$ decays, FV loop corrections to the flavor-conserving $Z \rightarrow \ell_i \ell_i$ decays, LEP searches, electroweak precision observables (EWPO), lepton number-changing decays such as $\ell_i \rightarrow 3\ell_j$, $\ell_i \rightarrow \ell_j \gamma$ decays, muon conversion in nuclei, and muonium-antimuonium oscillation. Additionally, we derive novel bounds from processes such as $\ell_i \rightarrow \ell_j + \text{inv.}$ decays, meson decays and from τ decays to $\mu(e) + \text{mesons}$.

In general, we find that bounds extracted from indirect searches are stronger than those from the LHC's direct searches by several orders of magnitude. Specifically, for the FV Z couplings to $\tau\mu$, we find that $\tau \rightarrow \mu\gamma$ provides the strongest constraints, reaching a level of $\mathcal{O}(10^{-5})$. Bounds from the decays $\tau \rightarrow 3\mu$ and $\tau \rightarrow \mu ee$ also impose strong constraints, at the level of $\mathcal{O}(10^{-4}) - \mathcal{O}(10^{-5})$, compared to $\mathcal{O}(10^{-3})$ from direct searches. Additionally, we find that bounds from FV leptonic meson decays can be as strong as $\mathcal{O}(10^{-2}) - \mathcal{O}(10^{-4})$, whereas bounds from τ decays involving mesons and from $\tau \rightarrow \mu + \text{inv.}$ could reach $\mathcal{O}(10^{-4}) - \mathcal{O}(10^{-5})$. Other constraints, such as those from electroweak precision observables (EWPO) and flavor-conserving Z decays, provide less stringent bounds. Finally, we find that future experiments on $\tau \rightarrow \mu\gamma$ could improve the bound to $\mathcal{O}(10^{-6})$.

As for the bounds on the FV Z couplings to τe , we find that τ decays to $3e$ and $\mu\mu e$ provide the strongest constraints, reaching $\mathcal{O}(10^{-7})$, compared to $\mathcal{O}(10^{-3})$ from direct searches. We also find that $\tau \rightarrow e\gamma$ can impose strong limits of $\mathcal{O}(10^{-5})$. Bounds from meson decays and from $\tau \rightarrow e + \text{inv.}$ can reach $\mathcal{O}(10^{-2}) - \mathcal{O}(10^{-4})$, whereas those from τ decays involving mesons can impose constraints at the level of $\mathcal{O}(10^{-4}) - \mathcal{O}(10^{-5})$. Other constraints, such as those from LEP searches and loop corrections to flavor-conserving Z decays to leptons, are much weaker and reach at best of $\mathcal{O}(10^{-2})$. Future experiments on $\tau \rightarrow 3e$ may improve the bound to $\mathcal{O}(10^{-8})$.

Finally, the strongest bounds on FV Z couplings to μe arise from the $\mu \rightarrow 3e$ decay, which reach $\mathcal{O}(10^{-11})$, compared to only $\mathcal{O}(10^{-4})$ from direct searches. Constraints from $\mu \rightarrow e + \text{inv.}$, $\mu \rightarrow e$ conversion and $\mu \rightarrow e\gamma$ are also stringent, reaching $\mathcal{O}(10^{-8}) - \mathcal{O}(10^{-11})$. Bounds from meson decays to μe can be as strong as $\mathcal{O}(10^{-2}) - \mathcal{O}(10^{-8})$, whereas other constraints, such as those from LEP searches, flavor-conserving Z decays, meson decays, and muonium-antimuonium oscillations, yield weaker bounds of at most $\mathcal{O}(10^{-2}) - \mathcal{O}(10^{-3})$. Future experiments, particularly on $\mu \rightarrow 3e$, could further improve the bound to $\mathcal{O}(10^{-13})$. In general, we find that the most promising experiments to search for FV in the Z interaction with leptons, include the decays of ℓ_i to $3\ell_j$, $\ell_j\gamma$ and $\ell_j + \text{inv.}$ in addition to muon conversion. Furthermore, we find that both meson decays and τ decays involving mesons are also promising channels to search for FV and deserve attention.

This paper is organized as follows: In Section II we present our framework for describing FV in the Z interaction with fermions. In Section III, we discuss all the bounds and projections in detail. We relegate some of the technical details to the appendices. We finally present our conclusions and future direction in Section IV.

II. THE FRAMEWORK

As alluded to above, in the SM, the Z sector is flavor-conserving. More specifically, the coupling of the Z boson to fermions can be written as

$$\mathcal{L}_{Zff}^{\text{SM}} = -Z_\mu \bar{f} \gamma^\mu (g_L^f P_L + g_R^f P_R) f, \quad (1)$$

where

$$g_L^f = \frac{g}{\cos \theta_W} (T_{fL}^3 - Q_f \sin^2 \theta_W), \quad g_R^f = \frac{-g}{\cos \theta_W} (Q_f \sin^2 \theta_W),$$

with T_{fL}^3 being the 3rd component of the weak isospin, θ_W being the weak mixing angle and with both g_L^f and g_R^f being real in the SM. Working in a bottom-up approach, it is fairly easy to generalize Eq. (1) to include FV simply by promoting $g_{L,R}^f$ to become non-diagonal matrices. As such, the FV version of Eq. (1) becomes

$$\mathcal{L}_{Zf_i f_j}^{\text{FV}} = -Z_\mu \bar{f}_i \gamma^\mu (g_L^{ij} P_L + g_R^{ij} P_R) f_j + h.c., \quad (2)$$

with the diagonal elements of the matrices $g_{L,R}^{ij}$ corresponding to the SM flavor-conserving couplings

$$g_L^{\text{SM}} = 2g_L^{ii} \equiv g_L^f, \quad g_R^{\text{SM}} = 2g_R^{ii} \equiv g_R^f, \quad (3)$$

where the factor of 2 is due the h.c. piece. In general, the elements of $g_{L,R}^{ij}$ can be complex, and need not be symmetric, however, we shall assume that they are symmetric for the sake of simplicity, but allow for the possibility that they could be complex. This assumption is plausible and does not represent much limitation. The Lagrangian in Eq. (2) is an EFT that arises from an unknown UV sector at some scale of NP Λ . However, we can match the BSM contributions to $g_{L,R}^{ij}$ to higher-dimensional operators in the SMEFT. For example, [33] studied FV Z decays to $\tau\mu$ and μe using the dimension-6 FV operators in the basis developed in [42]. However, here we find it more convenient to use the so-called Warsaw basis [43]. We point out that Z decays within the SMEFT were studied in [44], but with no treatment of FV. At dimension-6, the following FV operators can contribute to $g_{L,R}^{ij}$

$$\begin{aligned} \mathcal{O}_{\text{SMEFT}}^6 : & (H^\dagger i \overleftrightarrow{D}_\mu H) (\bar{\ell}_i \gamma^\mu \ell_j), (H^\dagger i \overleftrightarrow{D}_\mu^I H) (\bar{\ell}_i \sigma^I \gamma^\mu \ell_j), (H^\dagger i \overleftrightarrow{D}_\mu H) (\bar{e}_i \gamma^\mu e_j), \\ & (\bar{\ell}_i \sigma^{\mu\nu} e_j) (\sigma^I H W_{\mu\nu}^I), (\bar{\ell}_i \sigma^{\mu\nu} e_j) (H B_{\mu\nu}), \end{aligned} \quad (4)$$

where $i = j$ corresponds to flavor-conserving operators and $i \neq j$ to FV ones, $W_{\mu\nu}^I = \partial_\mu W_\nu^I - \partial_\nu W_\mu^I - g\epsilon^{IJK} W_\mu^J W_\nu^K$, $B_{\mu\nu} = \partial_\mu B_\nu - \partial_\nu B_\mu$, $H^\dagger i \overleftrightarrow{D}_\mu H = iH^\dagger (D_\mu - \overleftarrow{D}_\mu) H$, $H^\dagger i \overleftrightarrow{D}_\mu^I H = iH^\dagger (\sigma^I D_\mu - \overleftarrow{D}_\mu^I) H$

$\overleftarrow{D}_\mu \sigma^I)H$, and the covariant derivative is given by $D_\mu = \partial_\mu + \frac{i}{2}g'B_\mu + \frac{i}{2}gW_\mu^I\sigma^I$. Notice here that since these operators contribute to the off-diagonal FV elements of $g_{L,R}^{ij}$, as well as to the diagonal SM ones, the contributions to the SM couplings must be suppressed to satisfy the experimental constraints on $g_{L,R}$. Therefore, the Lagrangian in Eq. (2) involves some fine-tuning to keep the diagonal contributions suppressed while allowing for significant deviations in the off-diagonal ones. Such fine-tuning might appear unnatural, however, we show below that it is quite possible within the relevant FV dimension-6 SMEFT operators without radical assumptions.

Notice that the operators in Eq. (4) are in the unbroken phase. It is more convenient to work in the broken phase where the physical Z boson is manifest. The SMEFT operators in the broken phase were worked out in [45], and here we review their main results relevant to this paper, limiting ourselves to the gauge sector.

When including dimension-6 operators, the kinetic terms of the gauge bosons receive contributions from the two operators in the second line of Eq. (4) and thus must be normalized. In order to do so, the gauge fields and couplings in the unbroken phase are redefined as follows:

$$\begin{aligned} W_\mu^I &= \mathcal{W}_\mu^I(1 + C_{HW}v_T^2), \\ B_\mu^I &= \mathcal{B}_\mu^I(1 + C_{HB}v_T^2), \\ \bar{g}_1 &= g_1(1 + C_{HB}v_T^2), \\ \bar{g}_2 &= g_1(1 + C_{HW}v_T^2), \end{aligned} \tag{5}$$

where C_{HW} and C_{HB} are the Wilson coefficients of the two operators above and v_T is the total Higgs VEV including all contributions from dim-6 operators that contribute to the Higgs potential¹, which can be expressed as

$$v_T = \left(1 + \frac{3C_H v^3}{8\lambda}\right)v. \tag{6}$$

\mathcal{W}_μ^I and \mathcal{B}_μ can be rotated into the physical states as follows

$$\begin{pmatrix} \mathcal{Z}^\mu \\ \mathcal{A}^\mu \end{pmatrix} = \begin{pmatrix} \bar{c} - \frac{\epsilon}{2}\bar{s} & -\bar{s} + \frac{\epsilon}{2}\bar{c} \\ \bar{s} + \frac{\epsilon}{2}\bar{c} & \bar{c} + \frac{\epsilon}{2}\bar{s} \end{pmatrix} \begin{pmatrix} \mathcal{W}_3^\mu \\ \mathcal{B}^\mu \end{pmatrix}, \tag{7}$$

¹ The dim-6 operators that contribute to the Higgs VEV and kinetic terms are $\mathcal{L}_H^6 = C_H(H^\dagger H)^3 + C_{H\Box}(H^\dagger H)\Box(H^\dagger H) + C_{HD}(H^\dagger D^\mu H)^*(H^\dagger D_\mu H)$, where the first one contributes to the VEV, whereas the remaining two contribute to the kinetic term.

where $\epsilon = C_{HWB}v_T^2$ and²

$$\begin{aligned}\bar{c} &= \cos \bar{\theta} = \frac{\bar{g}_2}{\sqrt{\bar{g}_1^2 + \bar{g}_2^2}} \left[1 - \frac{\epsilon \bar{g}_1}{2 \bar{g}_2} \left(\frac{\bar{g}_2^2 - \bar{g}_1^2}{\bar{g}_2^2 + \bar{g}_1^2} \right) \right], \\ \bar{s} &= \sin \bar{\theta} = \frac{\bar{g}_1}{\sqrt{\bar{g}_1^2 + \bar{g}_2^2}} \left[1 + \frac{\epsilon \bar{g}_2}{2 \bar{g}_1} \left(\frac{\bar{g}_2^2 - \bar{g}_1^2}{\bar{g}_2^2 + \bar{g}_1^2} \right) \right].\end{aligned}\quad (8)$$

Furthermore, the mass and effective couplings of the physical \mathcal{Z}_μ get modified:

$$\begin{aligned}M_{\mathcal{Z}}^2 &= \frac{1}{4}(\bar{g}_1^2 + \bar{g}_2^2)v_T^2 \left(1 + \frac{1}{2}C_{HD}v_T^2 \right) + \frac{\epsilon}{2}\bar{g}_1\bar{g}_2v_T^2, \\ \bar{g}_Z &= \frac{\bar{e}}{\sin \bar{\theta} \cos \bar{\theta}} \left[1 + \left(\frac{\bar{g}_1^2 + \bar{g}_2^2}{2\bar{g}_1\bar{g}_2} \right) v_T^2 C_{HWB} \right], \\ \bar{e} &= \bar{g}_2 \sin \bar{\theta} - \frac{1}{2} \cos \bar{\theta} \bar{g}_2 v_T^2 C_{HWB}.\end{aligned}\quad (9)$$

Now, we have all the ingredients needed to extract the couplings of the physical \mathcal{Z} to the rest of the SM particles. For fermions, the dim-6 $\mathcal{Z}ff$ can be expressed as

$$\mathcal{L}_{\mathcal{Z}}^{(6)} = -\bar{g}_{\mathcal{Z}} \mathcal{Z}_\mu J_{\mathcal{Z}}^\mu, \quad (10)$$

where neglecting neutrinos, the neutral current $J_{\mathcal{Z}}^\mu$ is given by

$$\begin{aligned}J_{\mathcal{Z}}^\mu &= [Z_{eL}]_{ij} \bar{e}_{L_i} \gamma^\mu e_{L_j} + [Z_{eR}]_{ij} \bar{e}_{R_i} \gamma^\mu e_{R_j} + [Z_{uL}]_{ij} \bar{u}_{L_i} \gamma^\mu u_{L_j} \\ &+ [Z_{uR}]_{ij} \bar{u}_{R_i} \gamma^\mu u_{R_j} + [Z_{dL}]_{ij} \bar{d}_{L_i} \gamma^\mu d_{L_j} + [Z_{dR}]_{ij} \bar{d}_{R_i} \gamma^\mu d_{R_j},\end{aligned}\quad (11)$$

where i, j are generation indices, and the coefficients are given by

$$\begin{aligned}[Z_{eL}]_{ij} &= \left[\left(-\frac{1}{2} + \bar{s}^2 \right) \delta_{ij} - \frac{1}{2} v_T^2 C_{Hl}^{(1)} - \frac{1}{2} v_T^2 C_{Hl}^{(3)} \right], \\ [Z_{eR}]_{ij} &= \left[\bar{s}^2 \delta_{ij} - \frac{1}{2} v_T^2 C_{He} \right], \\ [Z_{uL}]_{ij} &= \left[\left(\frac{1}{2} - \frac{2}{3} \bar{s}^2 \right) \delta_{ij} - \frac{1}{2} v_T^2 C_{Hq}^{(1)} + \frac{1}{2} v_T^2 C_{Hq}^{(3)} \right], \\ [Z_{uR}]_{ij} &= \left[-\frac{2}{3} \bar{s}^2 \delta_{ij} - \frac{1}{2} v_T^2 C_{Hu} \right], \\ [Z_{dL}]_{ij} &= \left[\left(-\frac{1}{2} + \frac{1}{3} \bar{s}^2 \right) \delta_{ij} - \frac{1}{2} v_T^2 C_{Hq}^{(1)} - \frac{1}{2} v_T^2 C_{Hq}^{(3)} \right], \\ [Z_{dR}]_{ij} &= \left[\frac{1}{3} \bar{s}^2 \delta_{ij} - \frac{1}{2} v_T^2 C_{Hq} \right],\end{aligned}\quad (12)$$

² C_{HWB} is the coefficient of the SMEFT operator $H^\dagger \sigma^I W_{\mu\nu}^I B^{\mu\nu}$

and as usual, the FV coefficients are given by $i \neq j$, whereas the flavor-conserving ones by $i = j$; contribute to the SM couplings. Thus, it is possible to tune the diagonal contributions to zero while allowing the off-diagonal ones to be free parameters via an appropriate choice of the parameters. For example, if we set $C_H = C_{HB} = C_{HW} = C_{HWB} = 0$, then this implies that $v_T = v$, $\bar{g}_{1,2} = g_{1,2}$, $\bar{g}_Z = g_Z$, $\bar{\theta} = \theta_W$, $\mathcal{Z}^\mu = Z^\mu$, $\mathcal{A}^\mu = A^\mu$ and $M_Z = m_Z$, and setting $C_{ii}^{xx} = 0$ while allowing $C_{ij}^{xx} \neq 0$ for $i \neq j$ will introduce no contributions to the diagonal terms, while inducing non-vanishing contributions to the off-diagonal couplings. As a concrete example, consider the $Z\bar{e}e$ interaction

$$\mathcal{L}_{ee} = -g_Z Z_\alpha \left([Z_{e_L}]_{ij} \bar{e}_{L_i} \gamma^\alpha e_{L_j} + [Z_{e_R}]_{ij} \bar{e}_{R_i} \gamma^\alpha e_{R_j} \right), \quad (13)$$

with the coefficients given by the first and second lines of Eq. (12). If we set $C_{11}^{(1)} = C_{11}^{(3)} = C_{H_e} = 0$, then $[Z_{e_L}]_{11}$ and $[Z_{e_R}]_{11}$ will reduce to their SM values and the diagonal part of Eq. (13) reduces to the SM Lagrangian. On the other hand, allowing $C_{1i}^{(1)}$, $C_{1i}^{(3)}$, and $C_{H_e}^{1i}$ (for $i = 2, 3$) to have non-vanishing values will give rise to the off-diagonal interaction term

$$\mathcal{L}_{e\mu, e\tau} = -g_Z Z_\alpha \left([Z_{e_L}]_{12} \bar{e}_L \gamma^\alpha \mu_L + [Z_{e_R}]_{12} \bar{e}_R \gamma^\alpha \mu_R + h.c. \right) + (\mu \leftrightarrow \tau), \quad (14)$$

which can immediately be matched to Eq. (2). Another possibility is to simply absorb all diagonal dim-6 contributions in the definition of the SM couplings, however, this requires the assumptions that such contributions are all flavor-universal or very close to flavor-universal as the case in the SM. Thus to summarize, it is possible to suppress the contributions of higher-dimensional operators to the diagonal terms of $g_{L,R}^{ij}$ while allowing the off-diagonal ones to be sizable, albeit at the expense of some fine-tuning that will always be unavoidable.

III. BOUNDS ON THE FV Z INTERACTIONS

In this section, we will discuss the relevant constraints on the FV Z couplings to leptons. We postpone investigating FV in the quark sector to future work. Explicitly, we write the leptonic part of Eq. (2) as follows

$$\mathcal{L}_l = \mathcal{L}_l^{\text{SM}} - Z_\alpha \bar{\tau} \gamma^\alpha (g_L^{\tau\mu} P_L + g_R^{\tau\mu} P_R) \mu - Z_\alpha \bar{\tau} \gamma^\alpha (g_L^{\tau e} P_L + g_R^{\tau e} P_R) e - Z_\alpha \bar{\mu} \gamma^\alpha (g_L^{\mu e} P_L + g_R^{\mu e} P_R) e + h.c.. \quad (15)$$

This is the main formula we use throughout this paper to extract bounds on the FV Z couplings to leptons. All the bounds reported in this paper are given @90% CL. Tables I, II and III summarize the results, in addition to the plots in Fig. 10.

Channel	Couplings	Bounds	Projections
$Z \rightarrow \tau\mu$	$\sqrt{ g_L^{\tau\mu} ^2 + g_R^{\tau\mu} ^2}$	$< 2.35 \times 10^{-3}$	$< 2.91 \times 10^{-5}$
EWPO - U parameter	$\sqrt{ g_L^{\tau\mu} ^2 + g_R^{\tau\mu} ^2}$	< 0.2	-
$Z \rightarrow \mu^+\mu^-$	$\sqrt{g_L^2 g_L^{\tau\mu} ^2 + g_R^2 g_R^{\tau\mu} ^2}$	< 0.11	-
$Z \rightarrow \tau^+\tau^-$	$\sqrt{g_L^2 g_L^{\tau\mu} ^2 + g_R^2 g_R^{\tau\mu} ^2}$	< 0.12	-
$\tau \rightarrow \mu\gamma$	$\sqrt{g_L^2 g_L^{\tau\mu} ^2 + g_R^2 g_R^{\tau\mu} ^2}$	$< 2.85 \times 10^{-7}$	$< 4.4 \times 10^{-8}$
$\tau \rightarrow 3\mu$	$\sqrt{g_L^2 g_L^{\tau\mu} ^2 + g_R^2 g_R^{\tau\mu} ^2}$	$< 8.64 \times 10^{-7}$	$< 1.33 \times 10^{-7}$
$\tau \rightarrow \mu^- e^+ e^-$	$\sqrt{g_L^2 g_L^{\tau\mu} ^2 + g_R^2 g_R^{\tau\mu} ^2}$	$< 5.66 \times 10^{-7}$	-
$\tau \rightarrow \mu^+ e^- e^-$	$\sqrt{g_L^2 g_L^{\tau\mu} ^2 + g_R^2 g_R^{\tau\mu} ^2}$	$< 7.3 \times 10^{-7}$	-
$\tau \rightarrow \mu + \text{inv.}$	$\sqrt{ g_L^{\tau\mu} ^2 + g_R^{\tau\mu} ^2}$	$< 2.76 \times 10^{-4}$	-
$\Upsilon(1S) \rightarrow \tau\mu$	$\sqrt{ g_L^{\tau\mu} ^2 + g_R^{\tau\mu} ^2}$	< 0.11	-
$\Upsilon(2S) \rightarrow \tau\mu$	$\sqrt{ g_L^{\tau\mu} ^2 + g_R^{\tau\mu} ^2}$	$< 7.81 \times 10^{-2}$	-
$\Upsilon(3S) \rightarrow \tau\mu$	$\sqrt{ g_L^{\tau\mu} ^2 + g_R^{\tau\mu} ^2}$	$< 5.11 \times 10^{-2}$	-
$J/\psi \rightarrow \tau\mu$	$\sqrt{ g_L^{\tau\mu} ^2 + g_R^{\tau\mu} ^2}$	< 0.95	-
$B^0 \rightarrow \tau\mu$	$\sqrt{ g_L^{\tau\mu} ^2 + g_R^{\tau\mu} ^2}$	$< 3.42 \times 10^{-4}$	-
$B_s \rightarrow \tau\mu$	$\sqrt{ g_L^{\tau\mu} ^2 + g_R^{\tau\mu} ^2}$	$< 7.24 \times 10^{-3}$	-
$\tau \rightarrow \mu\rho^0$	$\sqrt{ g_L^{\tau\mu} ^2 + g_R^{\tau\mu} ^2}$	$< 5.5 \times 10^{-5}$	-
$\tau \rightarrow \mu\omega$	$\sqrt{ g_L^{\tau\mu} ^2 + g_R^{\tau\mu} ^2}$	$< 8.34 \times 10^{-5}$	-
$\tau \rightarrow \mu\phi$	$\sqrt{ g_L^{\tau\mu} ^2 + g_R^{\tau\mu} ^2}$	$< 6.12 \times 10^{-5}$	-
$\tau \rightarrow \mu\pi^0$	$\sqrt{ g_L^{\tau\mu} ^2 + g_R^{\tau\mu} ^2}$	$< 2.15 \times 10^{-4}$	-
$\tau \rightarrow \mu K_s^0$	$\sqrt{ g_L^{\tau\mu} ^2 + g_R^{\tau\mu} ^2}$	$< 8.92 \times 10^{-5}$	-
$\tau \rightarrow \mu\eta$	$\sqrt{ g_L^{\tau\mu} ^2 + g_R^{\tau\mu} ^2}$	$< 2.19 \times 10^{-4}$	2.72×10^{-5}
$\tau \rightarrow \mu\eta'$	$\sqrt{ g_L^{\tau\mu} ^2 + g_R^{\tau\mu} ^2}$	$< 4.8 \times 10^{-4}$	-

TABLE I: 90% CL bounds and projections on the leptonic next-to-minimal FV Z couplings to τ and μ .

A. Constraints from $Z \rightarrow \ell_i^\pm \ell_j^\mp$ Direct Searches

The first and most straightforward bound arises from the direct searches for FV Z decays, which have been updated recently by the LHC. This process can take place at tree-level and a simple calculation yields

$$\Gamma(Z \rightarrow \ell_i^\pm \ell_j^\mp) \simeq \frac{M_Z}{12\pi} \left(|g_L^{ij}|^2 + |g_R^{ij}|^2 \right), \quad (16)$$

where $\ell_{i,j} = \{e, \mu, \tau\}$ and we have dropped terms of $\mathcal{O}(m_{\ell_{i,j}}/M_Z)$. Notice here that there is a factor of 2 stemming from the hermitian conjugate part of the Lagrangian, since the experimental bound is given for $Z \rightarrow \ell^\pm \ell^\mp$. For the decay $Z \rightarrow \mu^\pm e^\mp$, the latest bounds can be found in [46] and read $\text{Br}(Z \rightarrow \mu^\pm e^\mp) < 2.62 \times 10^{-7}$ @95% CL. This can be translated into the 90% CL

Channel	Couplings	Bounds	Projections
$Z \rightarrow \tau e$	$\sqrt{ g_L^{\tau e} ^2 + g_R^{\tau e} ^2}$	$< 2.06 \times 10^{-3}$	$< 2.91 \times 10^{-5}$
EWPO - U parameter	$\sqrt{ g_L^{\tau e} ^2 + g_R^{\tau e} ^2}$	< 0.2	-
LEP($e^+e^- \rightarrow \tau^+\tau^-$)	$\sqrt{ g_L^{\tau e} ^2 + 0.91 g_R^{\tau e} ^2}$	$< 6.28 \times 10^{-2}$	-
$Z \rightarrow e^+e^-$	$\sqrt{g_L^2 g_L^{\tau e} ^2 + g_R^2 g_R^{\tau e} ^2}$	$< 8.43 \times 10^{-2}$	-
$Z \rightarrow \tau^+\tau^-$	$\sqrt{g_L^2 g_L^{\tau e} ^2 + g_R^2 g_R^{\tau e} ^2}$	< 0.12	-
$\tau \rightarrow e\gamma$	$\sqrt{g_L^2 g_L^{\tau e} ^2 + g_R^2 g_R^{\tau e} ^2}$	$< 2.53 \times 10^{-7}$	$< 9.84 \times 10^{-8}$
$\tau \rightarrow 3e$	$\sqrt{g_L^2 g_L^{\tau e} ^2 + g_R^2 g_R^{\tau e} ^2}$	$< 4.72 \times 10^{-9}$	$< 6.43 \times 10^{-10}$
$\tau \rightarrow \mu^-\mu^+e^-$	$\sqrt{g_L^2 g_L^{\tau e} ^2 + g_R^2 g_R^{\tau e} ^2}$	$< 3.34 \times 10^{-9}$	-
$\tau \rightarrow \mu^-\mu^-e^+$	$\sqrt{g_L^2 g_L^{\tau e} ^2 + g_R^2 g_R^{\tau e} ^2}$	$< 3.75 \times 10^{-9}$	-
$\tau \rightarrow e + \text{inv.}$	$\sqrt{ g_L^{\tau e} ^2 + g_R^{\tau e} ^2}$	$< 2.76 \times 10^{-4}$	-
$\Upsilon(2S) \rightarrow \tau e$	$\sqrt{ g_L^{\tau e} ^2 + g_R^{\tau e} ^2}$	$< 7.69 \times 10^{-2}$	-
$\Upsilon(3S) \rightarrow \tau e$	$\sqrt{ g_L^{\tau e} ^2 + g_R^{\tau e} ^2}$	$< 5.95 \times 10^{-2}$	-
$J/\psi \rightarrow \tau e$	$\sqrt{ g_L^{\tau e} ^2 + g_R^{\tau e} ^2}$	< 1.93	-
$B^0 \rightarrow \tau e$	$\sqrt{ g_L^{\tau e} ^2 + g_R^{\tau e} ^2}$	$< 3.66 \times 10^{-4}$	-
$B_s \rightarrow \tau e$	$\sqrt{ g_L^{\tau e} ^2 + g_R^{\tau e} ^2}$	$< 4.18 \times 10^{-2}$	-
$\tau \rightarrow e\rho^0$	$\sqrt{ g_L^{\tau e} ^2 + g_R^{\tau e} ^2}$	$< 6.26 \times 10^{-5}$	-
$\tau \rightarrow e\omega$	$\sqrt{ g_L^{\tau e} ^2 + g_R^{\tau e} ^2}$	$< 6.55 \times 10^{-5}$	-
$\tau \rightarrow e\phi$	$\sqrt{ g_L^{\tau e} ^2 + g_R^{\tau e} ^2}$	$< 5.71 \times 10^{-5}$	-
$\tau \rightarrow e\pi^0$	$\sqrt{ g_L^{\tau e} ^2 + g_R^{\tau e} ^2}$	$< 1.83 \times 10^{-4}$	-
$\tau \rightarrow eK_s^0$	$\sqrt{ g_L^{\tau e} ^2 + g_R^{\tau e} ^2}$	$< 9.48 \times 10^{-5}$	-
$\tau \rightarrow e\eta$	$\sqrt{ g_L^{\tau e} ^2 + g_R^{\tau e} ^2}$	$< 2.61 \times 10^{-4}$	-
$\tau \rightarrow e\eta'$	$\sqrt{ g_L^{\tau e} ^2 + g_R^{\tau e} ^2}$	$< 5.32 \times 10^{-4}$	-

TABLE II: 90% CL bounds and projections on the leptonic next-to-minimal FV Z couplings to τ and e .

bound³ $\sqrt{|g_L^{\mu e}|^2 + |g_R^{\mu e}|^2} < 4.72 \times 10^{-4}$. On the other hand, the bounds on $Z \rightarrow \tau^\pm \mu^\mp, \tau^\pm e^\mp$ can be found in [47] and when combined with previous bounds yield (also @95% CL) $\text{Br}(Z \rightarrow \tau^\pm \mu^\mp) < 6.5 \times 10^{-6}$ and $\text{Br}(Z \rightarrow \tau^\pm e^\mp) < 5 \times 10^{-6}$. These translate to $\sqrt{|g_L^{\tau\mu}|^2 + |g_R^{\tau\mu}|^2} < 2.35 \times 10^{-3}$ and $\sqrt{|g_L^{\tau e}|^2 + |g_R^{\tau e}|^2} < 2.06 \times 10^{-3}$, respectively.

The proposed FCC-ee collider measurements can improve the bounds on the FV Z decay to $\ell_i^\pm \ell_j^\mp$. The projections @95% CL are estimated to be $\text{Br}(Z \rightarrow \mu^\pm e^\mp) \simeq 10^{-8} - 10^{-10}$ and $\text{Br}(Z \rightarrow \tau^\pm e^\mp / \tau^\pm \mu^\mp) \simeq 10^{-9}$. These projections translate into the projected limits $\sqrt{|g_L^{\mu e}|^2 + |g_R^{\mu e}|^2} < 9.21 \times 10^{-6}$, $\sqrt{|g_L^{\tau\mu}|^2 + |g_R^{\tau\mu}|^2} < 2.91 \times 10^{-5}$ and $\sqrt{|g_L^{\tau e}|^2 + |g_R^{\tau e}|^2} < 2.91 \times 10^{-5}$, respectively, where

³ Whenever bounds are reported at a CL different from 90%, they are shifted to 90% to maintain consistency.

Channel	Couplings	Bounds	Projections
$Z \rightarrow \mu e$	$\sqrt{ g_L^{\mu e} ^2 + g_R^{\mu e} ^2}$	$< 4.72 \times 10^{-4}$	$< 9.21 \times 10^{-6}$
EWPO - U parameter	$\sqrt{ g_L^{\mu e} ^2 + g_R^{\mu e} ^2}$	< 0.2	-
LEP($e^+e^- \rightarrow \mu^+\mu^-$)	$\sqrt{ g_L^{\mu e} ^2 + 0.91 g_R^{\mu e} ^2}$	$< 5.62 \times 10^{-2}$	-
$Z \rightarrow e^+e^-$	$\sqrt{g_L^2 g_L^{\mu e} ^2 + g_R^2 g_R^{\mu e} ^2}$	$< 8.43 \times 10^{-2}$	-
$Z \rightarrow \mu^+\mu^-$	$\sqrt{g_L^2 g_L^{\mu e} ^2 + g_R^2 g_R^{\mu e} ^2}$	< 0.11	-
$\mu \rightarrow e\gamma$	$\sqrt{g_L^2 g_L^{\mu e} ^2 + g_R^2 g_R^{\mu e} ^2}$	$< 1.34 \times 10^{-12}$	$< 4.63 \times 10^{-13}$
$\mu \rightarrow 3e$	$\sqrt{g_L^2 g_L^{\mu e} ^2 + g_R^2 g_R^{\mu e} ^2}$	$< 7.17 \times 10^{-13}$	$< 7.17 \times 10^{-15}$
$\mu \rightarrow e$ conversion	$\sqrt{ g_L^{\mu e} ^2 + 0.74 g_R^{\mu e} ^2}$	$< 5.84 \times 10^{-11}$	$< 9.49 \times 10^{-13}$
$\mu \rightarrow e + \text{inv.}$	$\sqrt{ g_L^{\mu e} ^2 + g_R^{\mu e} ^2}$	$< 8.51 \times 10^{-8}$	$< 1.12 \times 10^{-9}$
$M - \bar{M}$ oscillation	$(g_L^{\mu e} ^2 + g_R^{\mu e} ^2)^2 + 6.5 g_L^{\mu e} ^2 g_R^{\mu e} ^2$ $-2.32(g_L^{\mu e} ^2 + g_R^{\mu e} ^2)\text{Re}(g_L^{\mu e}g_R^{\mu e*})$	$< 2.72 \times 10^{-6}$	-
$J/\psi \rightarrow \mu e$	$\sqrt{ g_L^{\mu e} ^2 + g_R^{\mu e} ^2}$	< 0.19	-
$\phi \rightarrow \mu e$	$\sqrt{ g_L^{\mu e} ^2 + g_R^{\mu e} ^2}$	< 42.93	-
$\eta \rightarrow \mu e$	$\sqrt{ g_L^{\mu e} ^2 + g_R^{\mu e} ^2}$	< 22.74	-
$\eta' \rightarrow \mu e$	$\sqrt{ g_L^{\mu e} ^2 + g_R^{\mu e} ^2}$	$< 2.16 \times 10^3$	-
$\pi^0 \rightarrow \mu e$	$\sqrt{ g_L^{\mu e} ^2 + g_R^{\mu e} ^2}$	$< 5.7 \times 10^{-2}$	-
$B^0 \rightarrow \mu e$	$\sqrt{ g_L^{\mu e} ^2 + g_R^{\mu e} ^2}$	$< 4.3 \times 10^{-5}$	-
$B_s \rightarrow \mu e$	$\sqrt{ g_L^{\mu e} ^2 + g_R^{\mu e} ^2}$	$< 8.21 \times 10^{-5}$	-
$D^0 \rightarrow \mu e$	$\sqrt{ g_L^{\mu e} ^2 + g_R^{\mu e} ^2}$	$< 4.51 \times 10^{-4}$	-
$K_L^0 \rightarrow \mu e$	$\sqrt{ g_L^{\mu e} ^2 + g_R^{\mu e} ^2}$	$< 6.57 \times 10^{-8}$	-

TABLE III: 90% CL bounds and projections on the leptonic FV Z couplings to μ and e .

we have used the strongest projection to set the limits on the FV Z couplings to μe .

B. LEP Constraints

LEP searches involving $e^+e^- \rightarrow \mu^+\mu^-, \tau^+\tau^-$ can be used to set limits on the FV Z couplings. These processes proceed via the s-channel and t-channel as shown in Fig. 1, with only the t-channel ones being FV. To find the cross-section, we express the total matrix element as follows

$$\mathcal{M} = \mathcal{M}_{\text{SM}} + \mathcal{M}_{\text{FV}}, \quad (17)$$

where \mathcal{M}_{SM} (\mathcal{M}_{FV}) is given by the s (t) channel. Working to the LO in $g_{L,R}^{el}$, it is easy to see that the leading FV contribution arises from the interferences terms between the SM and the FV

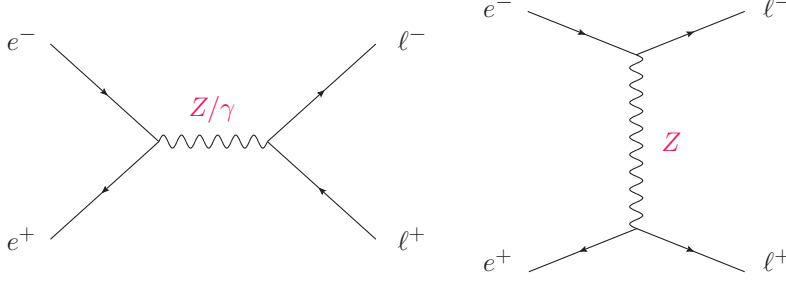


FIG. 1: LEP searches involving $e^+e^- \rightarrow \mu^+\mu^-, \tau^+\tau^-$. Only the t-channel could have FV couplings.

contributions $2\text{Re}(\mathcal{M}_{\text{SM}}\mathcal{M}_{\text{FV}}^*)$ and is given by

$$\delta\sigma_{\text{FV}}(e^+e^- \rightarrow \ell^-\ell^+) \simeq \frac{1}{16\pi s} \left[2 \left(1 + \frac{m_Z^2}{s} \right)^2 \log \left(1 + \frac{s}{m_Z^2} \right) - \left(3 + \frac{2m_Z^2}{s} \right) \right] \times \left(\left(g_L^2 \frac{s}{s - m_Z^2} + 4\pi\alpha \right) |g_L^{e\ell}|^2 + \left(g_R^2 \frac{s}{s - m_Z^2} + 4\pi\alpha \right) |g_R^{e\ell}|^2 \right). \quad (18)$$

This can be used to extract bounds on the FV Z couplings by demanding that the FV cross-sections in Eq. (18) be within the measured experimental uncertainties. The measured cross-section of these processes can be found in [48], where we find that the 1σ uncertainties on the cross-sections of $e^+e^- \rightarrow \mu^+\mu^-, \tau^+\tau^-$ are 0.088 pb and 0.11 pb, respectively at a COM energy of $\sqrt{s} = 207$ GeV. These measurements translate to the bounds $\sqrt{|g_L^{\mu e}|^2 + 0.91|g_R^{\mu e}|^2} < 5.62 \times 10^{-2}$ and $\sqrt{|g_L^{\tau e}|^2 + 0.91|g_R^{\tau e}|^2} < 6.28 \times 10^{-2}$. We point out that future e^+e^- colliders, such that ILC and the FCC-ee could potentially improve these limits.

C. Constraints from Loop Correction to the $Z \rightarrow \ell_i^+ \ell_i^-$ Decay

Although the Z decay to a pair of identical leptons does not have FV couplings at tree level, it nonetheless can receive contributions from FV couplings at 1-loop as shown in Fig. 2. Thus, it is possible to extract bounds on the FV Z couplings, especially since the branching ratios of the leptonic Z decays are well-measured. In our calculation, we drop terms of $O(m_{i,j}/m_Z)$. There are two types of FV corrections at 1-loop: Vertex corrections and leg corrections. As it turns out, the leading terms in the leg corrections are of $O(m_{i,j}/m_Z)$, thus we neglect them and only consider the vertex corrections. Using dimensional regularization in the \overline{MS} scheme, the leading FV vertex corrections read

$$\Gamma(Z \rightarrow \ell_i^+ \ell_i^-) \simeq \Gamma_0 + \frac{(16\pi^2 - 171)}{1536\pi^3} (g_L^2 |g_L^{ij}|^2 + g_R^2 |g_R^{ij}|^2) m_Z, \quad (19)$$

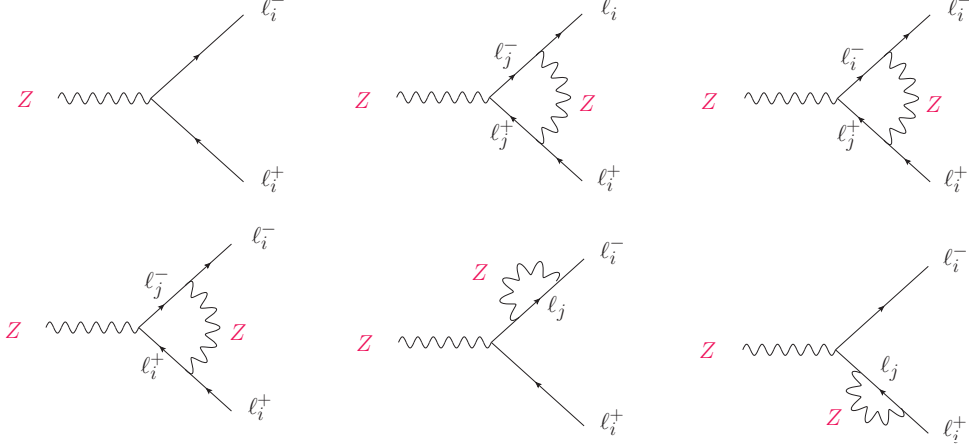


FIG. 2: Tree level and FV corrections to $Z \rightarrow \ell_i^+ \ell_i^-$ at one loop at LO in the FV couplings.

where $\Gamma_0 = \frac{1}{24\pi}(g_L^2 + g_R^2)m_Z$ is the tree level decay width. The latest bounds on the leptonic Z decays are given by [50]

$$\begin{aligned} \text{Br}(Z \rightarrow e^+e^-) &= (3363.2 \pm 4.2) \times 10^{-3}\%, \\ \text{Br}(Z \rightarrow \mu^+\mu^-) &= (3366.2 \pm 6.6) \times 10^{-3}\%, \\ \text{Br}(Z \rightarrow \tau^+\tau^-) &= (3369.6 \pm 8.3) \times 10^{-3}\%. \end{aligned} \quad (20)$$

Thus, to obtain the 90% CL bound, we require

$$\frac{\delta\Gamma(Z \rightarrow \ell_i^+ \ell_i^-)}{\Gamma_Z} < 1.7 \times \delta\Gamma_Z^{\text{Exp}}, \quad (21)$$

where we have introduced a factor of 1.7 to shift the bound to a 90% CL, since the experimental bounds are quoted with a scale factor of $s = 1.7$. For the first experimental bound, $\ell_i = e$, which means that FV bounds can be extracted by setting $\ell_j = \mu, \tau$. These are given by $\sqrt{g_L^2|g_L^{\mu e}|^2 + g_R^2|g_R^{\mu e}|^2} < 8.43 \times 10^{-2}$ and $\sqrt{g_L^2|g_L^{\tau e}|^2 + g_R^2|g_R^{\tau e}|^2} < 8.43 \times 10^{-2}$, respectively. Similarly, for the second bound we have $\ell_i = \mu$, which means that we can obtain FV bounds by setting $\ell_j = e, \tau$. The corresponding bounds are $\sqrt{g_L^2|g_L^{\mu e}|^2 + g_R^2|g_R^{\mu e}|^2} < 0.11$ and $\sqrt{g_L^2|g_L^{\tau \mu}|^2 + g_R^2|g_R^{\tau \mu}|^2} < 0.11$. Finally, setting $\ell_i = \tau$, the FV bounds are obtained with $\ell_j = \mu, e$, which read $\sqrt{g_L^2|g_L^{\tau e}|^2 + g_R^2|g_R^{\tau e}|^2} < 0.12$ and $\sqrt{g_L^2|g_L^{\tau \mu}|^2 + g_R^2|g_R^{\tau \mu}|^2} < 0.12$.

Notice that the bounds arising from $Z \rightarrow e^+e^-$ are stronger than these arising from $Z \rightarrow \mu^+\mu^-$, which are in turn stronger than these arising from $Z \rightarrow \tau^+\tau^-$, which is consistent with the experimental limits given in Eq. (20). However, these bounds are rather weak, which implies that this is not a promising channel to search for FV in the Z sector.

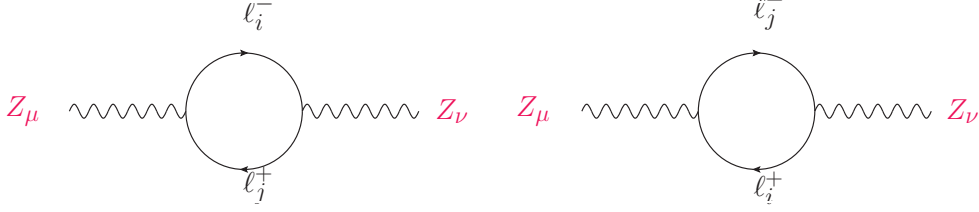


FIG. 3: FV corrections to Z self-energy $\Pi_{ZZ}^{\mu\nu}$.

D. Constraints from EWPO

FV Z couplings to fermions will contribute to the self-energy of the Z -propagator Π_{ZZ}^{ij} as shown in Fig. 3, which will impact EWPO. Thus, we can use the STU parameters to set bounds on the FV Z couplings. However, before we proceed with calculating Π_{ZZ}^{ij} , we should note that in the SM, the UV divergences cancel when adding Π_{ZZ} , Π_{WW} , $\Pi_{\gamma\gamma}$ and $\Pi_{\gamma Z}$, however, this cancellation no longer holds as we are ignoring any FV in the W/γ sectors. In the full theory, all such information should be available and the expectation is that UV divergences will cancel trivially. However, lacking such a UV-complete theory, we resort to dimensional regularization.

As only $\Pi_{ZZ}^{ij}(p^2 = 0)$ and $\Pi_{ZZ}^{ij}(p^2 = m_Z^2)$ will be needed to calculate the STU parameters, we evaluate the Feynman diagrams in Fig. 3 at these 2 points only, which greatly simplifies the integral over the Feynman parameters. We obtain

$$\Pi_{ZZ}^{ij}(0) \simeq \frac{m_i^2}{16\pi^2} \left(|g_L^{ij}|^2 + |g_R^{ij}|^2 \right) \left(1 - 2 \log \left(\frac{m_i^2}{\mu^2} \right) \right), \quad (22)$$

$$\Pi_{ZZ}^{ij}(m_Z^2) \simeq \frac{m_Z^2}{12\pi^2} \left(|g_L^{ij}|^2 + |g_R^{ij}|^2 \right) \left(\log \left(\frac{m_Z^2}{\mu^2} \right) - \frac{5}{3} + i\pi \right), \quad (23)$$

where m_i is the mass of the heavier particle in the loop and μ is the renormalization scale. Here, we set $\mu^2 = m_Z^2$ as the STU parameters are measured at the Z -pole (see for instance [49]). Assuming that the other propagators do not change, the STU parameters read

$$T = -\frac{1}{\alpha m_Z^2} \Pi_{ZZ}^{ij}(0), \quad (24)$$

$$S = -U = \frac{4 \cos^2 \theta_W \sin^2 \theta_W}{\alpha m_Z^2} \left(\Pi_{ZZ}^{ij}(m_Z^2) - \Pi_{ZZ}^{ij}(0) \right). \quad (25)$$

Notice that α here is evaluated at the Z pole and thus is equal to $1/128.99$. The latest bounds on the STU parameters read [50]

$$S = 0.02 \pm 0.1, \quad T = 0.07 \pm 0.12, \quad U = 0.00 \pm 0.09, \quad (26)$$

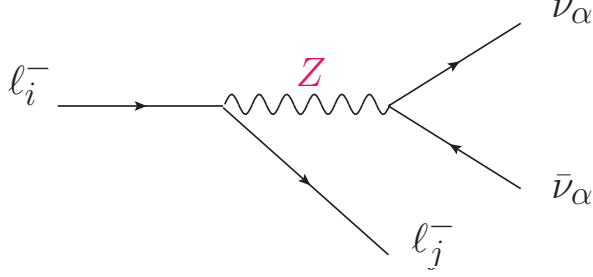


FIG. 4: The decay $l_i \rightarrow l_j + \text{inv.}$ through a FV Z . Here, we sum over all neutrino flavors $\alpha = e, \mu, \tau$.

and can be translated into bounds on the FV Z couplings. The strongest bounds arise from the U parameter, which reads

$$\sqrt{|g_L^{ij}|^2 + |g_R^{ij}|^2} < 0.2, \quad (27)$$

where $i, j = \{e, \mu, \tau\}$.⁴ Here too, we find that the bounds are rather weak, and thus EWPO are not the optimal way to search for FV in the Z sector.

E. Constraints from the decay $l_i \rightarrow l_j + \text{inv.}$

One of the novel bounds on the FV Z interactions can be obtained from the searches $\tau \rightarrow \mu \bar{\nu} \nu$, $\tau \rightarrow e \bar{\nu} \nu$, and $\mu \rightarrow e \bar{\nu} \nu$, which have the signature $l_i \rightarrow l_j + \cancel{E}$. A FV Z can contribute to these process through the diagram shown in Fig. 4. In calculating this decay, we have to sum over 3 neutrino flavors, which are all indistinguishable and appear as missing energy. As $m_\tau \gg m_\mu \gg m_e$, we can treat the final state particles including l_j as massless. In this approximation, decay width is given by

$$\Gamma(l_i \rightarrow l_j + \text{inv.}) \simeq \frac{g^2 m_i}{3072 \pi^3 \cos^2 \theta_W} (|g_L^{ij}|^2 + |g_R^{ij}|^2) \left[\left(\frac{6 - 3\lambda - \lambda^2}{\lambda} \right) + 6 \frac{(1 - \lambda)}{\lambda^2} \log(1 - \lambda) \right], \quad (28)$$

$$\simeq \frac{g^2 m_i^5}{6144 \pi^3 \cos^2 \theta_W m_z^4} (|g_L^{ij}|^2 + |g_R^{ij}|^2), \quad (29)$$

where $\lambda = \frac{m_i^2}{m_z^2}$. The TWIST collaboration reported bounds on $\mu^+ \rightarrow e^+ X^0$ [51], with X^0 being an invisible vector boson. The limit is given by $\text{Br}(\mu^+ \rightarrow e^+ X^0) < 5.8 \times 10^{-5}$, which translates to $\sqrt{|g_L^{\mu e}|^2 + |g_R^{\mu e}|^2} < 8.51 \times 10^{-8}$. On the other hand, the Belle experiment reported the following

⁴ Notice that in principle, the STU parameters will receive contributions from all FV couplings $g_{L,R}^{\tau\mu}$, $g_{L,R}^{\tau e}$, and $g_{L,R}^{\mu e}$ at the same time, however, to set an upper bound on each one, the other two are set to 0.

bounds on $\tau \rightarrow \mu X^0, eX^0$ [52, 53]: $\text{Br}(\tau \rightarrow \mu X^0) < (1.7 - 4.3) \times 10^{-8}$ and $\text{Br}(\tau \rightarrow eX^0) < (1.7 - 2.4) \times 10^{-8}$. Taking the lower limits of both bounds, they translate to $\sqrt{|g_L^{\tau\mu}|^2 + |g_R^{\tau\mu}|^2} < 2.76 \times 10^{-4}$ and $\sqrt{|g_L^{\tau e}|^2 + |g_R^{\tau e}|^2} < 2.76 \times 10^{-4}$, respectively. These bounds are quite significant, and in the case of the Z couplings to μe , they could compete with the classically most stringent bounds from $\ell_i \rightarrow \ell_j \gamma$ and $\ell_i \rightarrow 3\ell_j$ (see below). Therefore, these searches furnish a promising venue for searching for FV in the Z sector.

We point that the Mu3e experiment is projected to improve the bounds on $\mu \rightarrow eX^0$ to reach $O(10^{-8})$, which would improve the bound to $\sqrt{|g_L^{\mu e}|^2 + |g_R^{\mu e}|^2} < 1.12 \times 10^{-9}$.

F. Constraints from $\ell_i \rightarrow \ell_j \gamma$

A FV Z can contribute to the FV decay $\ell_i \rightarrow \ell_j \gamma$ through the Feynman diagrams shown in Fig. 5, where $\ell_i \neq \ell_j$. In addition to these vertex corrections, there are additional contributions where the photon is radiated from the initial and final state leptons, however, these diagrams are subleading and we neglect them here. We relegate the detailed calculation to Appendix A. Neglecting terms of $O(m_{i,j}/m_Z)$, the decay width is given by

$$\Gamma(\ell_i \rightarrow \ell_j \gamma) \simeq \alpha m_i \left(\frac{3}{32\pi^2} \right)^2 \left(g_L^2 |g_L^{ij}|^2 + g_R^2 |g_R^{ij}|^2 \right). \quad (30)$$

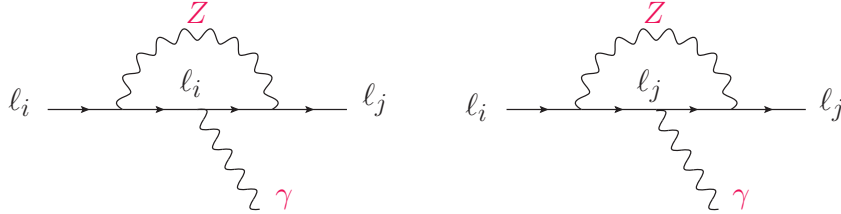


FIG. 5: The leading contributions to $\ell_i \rightarrow \ell_j \gamma$. Other contribution where γ is radiated from the initial or final states are subleading.

The most recent bounds on the $\tau \rightarrow \mu \gamma$ decay is given by $\text{Br}(\tau \rightarrow \mu \gamma) < 4.2 \times 10^{-8}$ [50]. This translates to $\sqrt{g_L^2 |g_L^{\tau\mu}|^2 + g_R^2 |g_R^{\tau\mu}|^2} < 2.85 \times 10^{-7}$. Similarly, the bounds on the $\tau \rightarrow e \gamma$ and $\mu \rightarrow e \gamma$ decays are given by $\text{Br}(\tau \rightarrow e \gamma) < 3.3 \times 10^{-8}$ and $\text{Br}(\mu \rightarrow e \gamma) < 4.2 \times 10^{-13}$ [50], which lead to the FV bounds $\sqrt{g_L^2 |g_L^{\tau e}|^2 + g_R^2 |g_R^{\tau e}|^2} < 2.53 \times 10^{-7}$ and $\sqrt{g_L^2 |g_L^{\mu e}|^2 + g_R^2 |g_R^{\mu e}|^2} < 1.34 \times 10^{-12}$. We can see that these bounds are quite stringent, making this channel one of the best places to search for FV in the Z sector.

The Belle II experiment is expected to improve the bounds by about an order of magnitude. Specifically, the projected Belle II bounds are expected to be $\text{Br}(\tau \rightarrow \mu \gamma) < 1 \times 10^{-9}$, $\text{Br}(\tau \rightarrow$

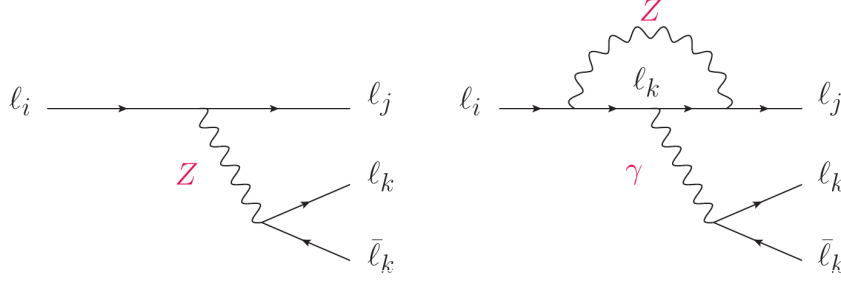


FIG. 6: The leading diagram for the process $l_i \rightarrow l_k + \bar{l}_k + l_j$.

$e\gamma) < 5 \times 10^{-9}$ and $\text{Br}(\mu \rightarrow e\gamma) < 5 \times 10^{-14}$, which would yield the bounds $\sqrt{g_L^2 |g_L^{\tau\mu}|^2 + g_R^2 |g_R^{\tau\mu}|^2} < 4.4 \times 10^{-8}$, $\sqrt{g_L^2 |g_L^{\tau e}|^2 + g_R^2 |g_R^{\tau e}|^2} < 9.84 \times 10^{-8}$, and $\sqrt{g_L^2 |g_L^{\mu e}|^2 + g_R^2 |g_R^{\mu e}|^2} < 4.63 \times 10^{-13}$, respectively.

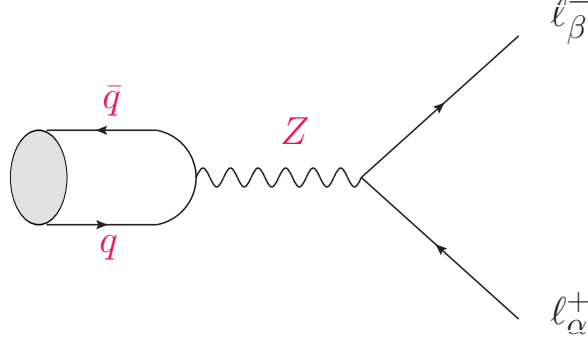
G. Constraints from $l_i \rightarrow l_j + l_k + \bar{l}_k$

Stringent constraints on the FV Z couplings can be obtained from the decays $l_i \rightarrow l_j + l_k + \bar{l}_k$ where l_j may or may not be identical to l_k . The leading contributions to these processes are shown in Fig. 6.

Notice that for the diagram on the right, it is possible to integrate out the loop and write it as an effective interaction at tree level. This can be achieved by utilizing the results of $l_i \rightarrow l_j \gamma$ (see Eq. (A3)). We present the full calculation in Appendix B. Explicit calculation shows that the loop calculation on the right dominates the one on the left by orders of magnitude in spite of the loop factor. The reason for this is the heavy mass in the Z propagator which suppresses the amplitude significantly enough to compensate for the loop factor. Thus, we neglect the contribution from this diagram. Assuming $m_i \gg m_j, m_k$, which is a valid assumption for the decays considered, we can treat the final state particles as massless. We only keep the mass of l_k to avoid any IR divergence in the second diagram. With these approximations, the decay width simplifies greatly and can be approximated as

$$\Gamma(l_i \rightarrow l_j l_k \bar{l}_k) \simeq \frac{3\alpha^2}{2048\pi^5 S} \frac{m_i^3}{m_k^2} \left(g_L^2 |g_L^{ij}|^2 + g_R^2 |g_R^{ij}|^2 \right), \quad (31)$$

where $S = 2$ is a possible symmetry factor if two of the final state particles are identical. Now, we can utilize the experimental bounds to set limits on the FV Z couplings. The first bound we consider is on the decay $\tau \rightarrow 3\mu$. The experimental limit is given by $\text{Br}(\tau \rightarrow 3\mu) < 2.1 \times 10^{-8}$ [50], which translates to $\sqrt{g_L^2 |g_L^{\tau\mu}|^2 + g_R^2 |g_R^{\tau\mu}|^2} < 8.64 \times 10^{-7}$. Bounds on the same coupling combinations can be obtained from the experimental limit $\text{Br}(\tau \rightarrow \mu^- e^+ e^-) < 1.8 \times 10^{-8}$, and $\text{Br}(\tau \rightarrow \mu^+ e^- e^-) <$

FIG. 7: FV meson decays mediated by the Z boson.

1.5×10^{-8} [50], which yield $\sqrt{g_L^2 |g_L^{\tau\mu}|^2 + g_R^2 |g_R^{\tau\mu}|^2} < 5.66 \times 10^{-7}$ and $\sqrt{g_L^2 |g_L^{\tau\mu}|^2 + g_R^2 |g_R^{\tau\mu}|^2} < 7.3 \times 10^{-7}$, respectively. To obtain bounds on the τe couplings, we use the experimental bounds on $\text{Br}(\tau \rightarrow 3e) < 2.7 \times 10^{-8}$, $\text{Br}(\tau \rightarrow \mu^+ \mu^- e^-) < 2.7 \times 10^{-8}$ and $\text{Br}(\tau \rightarrow \mu^- \mu^- e^+) < 1.7 \times 10^{-8}$ [50], which yield the bounds $\sqrt{g_L^2 |g_L^{\tau e}|^2 + g_R^2 |g_R^{\tau e}|^2} < 4.72 \times 10^{-9}$, $\sqrt{g_L^2 |g_L^{\tau e}|^2 + g_R^2 |g_R^{\tau e}|^2} < 3.34 \times 10^{-9}$ and $\sqrt{g_L^2 |g_L^{\tau e}|^2 + g_R^2 |g_R^{\tau e}|^2} < 3.75 \times 10^{-9}$, respectively. Finally, the experimental measurement of $\text{Br}(\mu \rightarrow 3e) < 1 \times 10^{-12}$ [50] give the bound $\sqrt{g_L^2 |g_L^{\mu e}|^2 + g_R^2 |g_R^{\mu e}|^2} < 7.17 \times 10^{-13}$. We can see that for each combination of couplings, bounds arising from different searches are close to one another, however, the bounds arising from mixed final states are slightly stronger than those obtained from identical final states.

In general, $\ell_i \rightarrow 3\ell_j$ decays are one of the most promising channels for searching for FV, with future experiments planned to take place. The Belle II experiment is expected to provide stronger bounds on these decays. In particular, the projected Belle II bound on $\text{Br}(\tau \rightarrow 3\mu)$ is expected to be 5×10^{-10} , which translates into $\sqrt{g_L^2 |g_L^{\tau\mu}|^2 + g_R^2 |g_R^{\tau\mu}|^2} < 1.33 \times 10^{-7}$. Similarly, the projected bounds on $\text{Br}(\tau \rightarrow 3e)$ and $\text{Br}(\mu \rightarrow 3e)$ are 5×10^{-10} and 1×10^{-16} , respectively, which become $\sqrt{g_L^2 |g_L^{\tau e}|^2 + g_R^2 |g_R^{\tau e}|^2} < 6.43 \times 10^{-10}$ and $\sqrt{g_L^2 |g_L^{\mu e}|^2 + g_R^2 |g_R^{\mu e}|^2} < 7.17 \times 10^{-15}$, respectively.

H. Constrains from FV Meson Decays

It was suggested in [56] (see also [57]) that experimental bounds on FV meson decays $M \rightarrow \ell_i \ell_j$ can be used to set bounds on the FV Wilson coefficients in an EFT. Such decays can also be used to constrain the FV Z couplings directly by considering the diagram in Fig. 7. As this decay is mediated by a vector meson, we can utilize the technique of current algebra, and write the interaction of the meson with the Z boson as

$$\mathcal{L}_{\text{int}} = \frac{e}{\sin \theta_W} Z_\mu J_Z^\mu, \quad (32)$$

where

$$J_Z^\mu = \sum_i \left[\frac{1}{\cos \theta_W} \bar{\psi}_i \gamma^\mu T^3 \psi_i - \frac{\sin^2 \theta_W}{\cos \theta_W} Q_i \bar{\psi}_i \gamma^\mu \psi_i \right], \quad (33)$$

and the sum is over all quarks. Thus, in the language of the current algebra, we can simply express the matrix element as follows

$$\mathcal{M} = \frac{ie}{\sin \theta_W} \langle 0 | J_Z^\mu | M(p) \rangle \left(\frac{g_{\mu\nu} - \frac{1}{m_Z^2} p_\mu p_\nu}{p^2 - m_Z^2} \right) \bar{u}(k_1) \gamma^\nu (g_L^{ij*} P_L + g_R^{ij*} P_R) v(k_2), \quad (34)$$

where p is the momentum of the meson. As we can see, the neutral vector current J_Z^μ allows the meson to turn into a Z boson, which in turn can decay via a FV interaction to leptons of different flavors. In general, the QCD matrix element is measured experimentally in terms of the decay constant and it depends on the type of mesons. For vector mesons, which are mesons with quantum numbers $J^{pc} = 1^{--}$, the QCD matrix element can be expressed as

$$\langle 0 | J_Z^\mu | V(q) \rangle = f_V m_V \epsilon^\mu(p), \quad (35)$$

where f_V is the decay constant and m_V is the mass of the vector meson. This can be used in Eq. (34) to find the decay width. Assuming without loss of generality that $m_i > m_j$ and dropping m_j since $m_\tau \gg m_\mu \gg m_e$, we find

$$\Gamma(V \rightarrow \bar{\ell}_i \ell_j) \simeq \frac{e^2 f_V^2 m_V^3}{48\pi \sin^2 \theta_W m_Z^4} \left(|g_L^{ij}|^2 + |g_R^{ij}|^2 \right) \left[1 - \frac{m_V^2}{m_Z^2} \right]^{-2} \left[1 - \frac{m_i^2}{m_V^2} \right]^2 \left[2 + \frac{m_i^2}{m_V^2} \right]. \quad (36)$$

The vector mesons for which experimental bounds on leptonic FV decays exist are: $\Upsilon(1S)$, $\Upsilon(2S)$, $\Upsilon(3S)$, J/ψ and ϕ . The relevant information of these mesons, including their masses, decay constant and decay widths, are provided in Table IV. The latest bound on the FV decays of all of these mesons can be found in [50]. For $\Upsilon(1S)$, the bound is given by $\text{Br}(\Upsilon(1S) \rightarrow \tau\mu) < 6 \times 10^{-6}$, which translate into the bound $\sqrt{|g_L^{\tau\mu}|^2 + |g_R^{\tau\mu}|^2} < 0.11$. Similarly, the FV limits from $\Upsilon(2S)$ are given by $\text{Br}(\Upsilon(2S) \rightarrow \tau\mu) < 3.3 \times 10^{-6}$ and $\text{Br}(\Upsilon(2S) \rightarrow \tau e) < 3.2 \times 10^{-6}$, which translate to $\sqrt{|g_L^{\tau\mu}|^2 + |g_R^{\tau\mu}|^2} < 7.81 \times 10^{-2}$ and $\sqrt{|g_L^{\tau e}|^2 + |g_R^{\tau e}|^2} < 7.69 \times 10^{-2}$, respectively. The experimental bounds from $\Upsilon(3S)$ read $\text{Br}(\Upsilon(3S) \rightarrow \tau\mu) < 3.1 \times 10^{-6}$ and $\text{Br}(\Upsilon(3S) \rightarrow \tau e) < 4.2 \times 10^{-6}$ from which we obtain $\sqrt{|g_L^{\tau\mu}|^2 + |g_R^{\tau\mu}|^2} < 5.11 \times 10^{-2}$ and $\sqrt{|g_L^{\tau e}|^2 + |g_R^{\tau e}|^2} < 5.95 \times 10^{-2}$, respectively. The experimental measurements of the FV decay of J/ψ are given by $\text{Br}(J/\psi \rightarrow \tau\mu) < 2 \times$

Meson	m_V	Γ_{M_V}	f_V
$\Upsilon(1S)$	9.4603	5.402×10^{-5}	0.649
$\Upsilon(2S)$	10.02326	3.198×10^{-5}	0.481
$\Upsilon(3S)$	10.3552	2.032×10^{-5}	0.539
J/ψ	3.0969	9.29×10^{-5}	0.418
ϕ	1.019461	4.249×10^{-3}	0.241
ρ	0.77526	0.1478	0.2094
ω	0.78266	8.68×10^{-3}	0.2094

TABLE IV: Mass, decay width and decay constant of the relevant vector mesons. All values are in GeV.

10^{-6} , $\text{Br}(J/\psi \rightarrow \tau e) < 8.3 \times 10^{-6}$ and $\text{Br}(J/\psi \rightarrow \mu e) < 1.6 \times 10^{-7}$, from which we obtain $\sqrt{|g_L^{\tau\mu}|^2 + |g_R^{\tau\mu}|^2} < 0.95$, $\sqrt{|g_L^{\tau e}|^2 + |g_R^{\tau e}|^2} < 1.93$ and $\sqrt{|g_L^{\mu e}|^2 + |g_R^{\mu e}|^2} < 0.19$, respectively. Finally, the bounds on the decay of ϕ is given by $\text{Br}(\phi \rightarrow \mu e) < 2 \times 10^{-6}$, which translate to the rather weak bound $\sqrt{|g_L^{\mu e}|^2 + |g_R^{\mu e}|^2} < 42.93$. The last bound seems to indicate that perturbativity is lost, however, the experimental limits are simply not strong enough to yield a meaningful bound.

Next, we turn our attention to pseudoscalar mesons⁵, which are mesons with quantum numbers $J^{pc} = 0^{-+}$. Table V contains all the relevant information for these mesons. The QCD matrix element can be expressed as

$$\langle 0 | J_Z^\mu | P(p) \rangle = -i f_P p^\mu, \quad (37)$$

which when used in Eq. (34) yields the decay width

$$\Gamma(P \rightarrow \ell_i \ell_j) \simeq \frac{n e^2 f_P^2}{16\pi \sin^2 \theta_W} \frac{m_V m_i^2}{m_Z^4} \left(|g_L^{ij}|^2 + |g_R^{ij}|^2 \right) \left[1 - \frac{m_i^2}{m_Z^2} \right]^2, \quad (38)$$

where $n = 2$ for $P = \pi^0, \eta, \eta'$ and $n = 1$ for all other mesons, since for the former mesons, experimental bounds are quoted on $\ell_i^\pm \ell_j^\mp + \ell_i^\mp \ell_j^\pm$, and thus there is an additional factor of 2 arising from the h.c. part of the Lagrangian. The experimental bounds on the FV decays of η, η' and π^0 are given by $\text{Br}(\eta \rightarrow \mu e) < 6 \times 10^{-6}$, $\text{Br}(\eta \rightarrow \mu e) < 4.7 \times 10^{-4}$ and $\text{Br}(\pi^0 \rightarrow \mu e) < 3.6 \times 10^{-6}$, respectively [50]. They translate to the following bounds $\sqrt{|g_L^{\mu e}|^2 + |g_R^{\mu e}|^2} < 22.72$, $\sqrt{|g_L^{\mu e}|^2 + |g_R^{\mu e}|^2} < 2.16 \times 10^3$ and $\sqrt{|g_L^{\mu e}|^2 + |g_R^{\mu e}|^2} < 5.7 \times 10^{-2}$, respectively, and we can see that the experimental bounds from the decay of η and η' are too weak to be meaningful, unlike the bounds from the decay of π^0 .

⁵ The only scalar meson that has FV bounds is the f^0 meson, however, we were unable to find a measured value of its decay constant.

Meson	m_P	Γ_{M_P}	f_P
η	0.547862	1.31×10^{-6}	0.108
η'	0.95778	1.88×10^{-4}	0.089
π^0	0.1349768	7.80421×10^{-9}	0.13041
B_d	5.27972	4.33681×10^{-13}	0.186
B_s	5.36693	4.30841×10^{-13}	0.224
D^0	1.86484	1.60345×10^{-12}	0.2074
K_L^0	0.497611	1.28596×10^{-17}	0.155
K_S^0	0.497611	7.3475×10^{-15}	0.155

TABLE V: Mass, decay width and decay constant of the relevant pseudo-scalar mesons. All values are in GeV.

Next, we consider the FV decays from B mesons. The limits on the FV decays of B_d are given by [50] $\text{Br}(B_d \rightarrow \tau\mu) < 1.4 \times 10^{-5}$, $\text{Br}(B_d \rightarrow \tau e) < 1.6 \times 10^{-5}$ and $\text{Br}(B_d \rightarrow \mu e) < 1 \times 10^{-9}$, which translate to $\sqrt{|g_L^{\tau\mu}|^2 + |g_R^{\tau\mu}|^2} < 3.42 \times 10^{-4}$, $\sqrt{|g_L^{\tau e}|^2 + |g_R^{\tau e}|^2} < 3.66 \times 10^{-4}$ and $\sqrt{|g_L^{\mu e}|^2 + |g_R^{\mu e}|^2} < 4.3 \times 10^{-5}$. Similarly, the experimental limits on the FV decays of B_s are given by $\text{Br}(B_s \rightarrow \tau\mu) < 4.2 \times 10^{-4}$, $\text{Br}(B_s \rightarrow \tau e) < 1.4 \times 10^{-3}$ and $\text{Br}(B_s \rightarrow \mu e) < 5.4 \times 10^{-9}$ [50], which yield the bounds $\sqrt{|g_L^{\tau\mu}|^2 + |g_R^{\tau\mu}|^2} < 7.24 \times 10^{-3}$, $\sqrt{|g_L^{\tau e}|^2 + |g_R^{\tau e}|^2} < 4.18 \times 10^{-2}$ and $\sqrt{|g_L^{\mu e}|^2 + |g_R^{\mu e}|^2} < 8.21 \times 10^{-5}$, respectively.

Finally, we consider the FV decays of the neutral mesons D^0 and K_L^0 . The experimental limits are given by $\text{Br}(D^0 \rightarrow \mu e) < 1.3 \times 10^{-8}$ and $\text{Br}(K_L^0 \rightarrow \mu e) < 4.7 \times 10^{-12}$, which translate to $\sqrt{|g_L^{\mu e}|^2 + |g_R^{\mu e}|^2} < 4.51 \times 10^{-4}$ and $\sqrt{|g_L^{\mu e}|^2 + |g_R^{\mu e}|^2} < 6.57 \times 10^{-8}$ respectively.

We can see from the above constraints, that meson decays can provide relatively strong constraints that are more stringent than direct searches, however, they fall short of competing with bound obtained from the usual channels, like $\ell_i \rightarrow \ell_j \gamma$ and $\ell_i \rightarrow 3\ell_j$. Nonetheless, searches for FV meson decays remain promising as potential channels to search for FV in the Z sector, and thus merit further interest.

I. $\tau \rightarrow \mu(e) + \text{Meson Decays}$

The same treatment introduced in the previous section can be used to set bounds on FV τ decays to a muon or an electron together with a meson. Such decays proceed via a diagram like Fig. 7 in reverse, with the initial state being $\ell_i = \tau$, and the final state being $\ell_j = \mu, e + \text{meson}$. The same current algebra technique can be used, and the results are quite similar. In our calculation we drop

m_j as usual. The decay width involving a vector meson is given by

$$\Gamma(\tau \rightarrow \ell V) \simeq \frac{e^2 f_V^2 m_\tau^3}{32\pi \sin^2 \theta_W m_Z^4} \left(|g_L^{\tau\ell}|^2 + |g_R^{\tau\ell}|^2 \right) \left[1 - \frac{m_V^2}{m_\tau^2} \right]^2 \left[1 + \frac{2m_V^2}{m_\tau^2} \right] \left[1 - \frac{m_V^2}{m_Z^2} \right]^{-2}. \quad (39)$$

The latest experimental measurements of the FV τ decays to $\mu, e + \text{meson}$ can be found in [50]. For decays involving the ρ^0 meson, the experimental measurements are given by $\text{Br}(\tau \rightarrow \mu\rho^0) < 1.7 \times 10^{-8}$ and $\text{Br}(\tau \rightarrow e\rho^0) < 2.2 \times 10^{-8}$, which translate to the limits $\sqrt{|g_L^{\tau\mu}|^2 + |g_R^{\tau\mu}|^2} < 5.5 \times 10^{-5}$ and $\sqrt{|g_L^{\tau e}|^2 + |g_R^{\tau e}|^2} < 6.26 \times 10^{-5}$, respectively. The experimental measurements involving decays to the ω meson read $\text{Br}(\tau \rightarrow \mu\omega) < 3.9 \times 10^{-8}$ and $\text{Br}(\tau \rightarrow e\omega) < 2.4 \times 10^{-8}$, which yield the bounds $\sqrt{|g_L^{\tau\mu}|^2 + |g_R^{\tau\mu}|^2} < 8.34 \times 10^{-5}$ and $\sqrt{|g_L^{\tau e}|^2 + |g_R^{\tau e}|^2} < 6.55 \times 10^{-5}$. Finally, the experimental limits on the decays involving the ϕ meson are given by $\text{Br}(\tau \rightarrow \mu\phi) < 2.3 \times 10^{-8}$ and $\text{Br}(\tau \rightarrow e\phi) < 2 \times 10^{-8}$, which translate to $\sqrt{|g_L^{\tau\mu}|^2 + |g_R^{\tau\mu}|^2} < 6.12 \times 10^{-5}$ and $\sqrt{|g_L^{\tau e}|^2 + |g_R^{\tau e}|^2} < 5.71 \times 10^{-5}$, respectively.

Next, we turn to τ decays involving pseudoscalar mesons. The decay width of these processes is given by

$$\Gamma(\tau \rightarrow \ell P) \simeq \frac{e^2 f_P^2 m_\tau^3}{32\pi \sin^2 \theta_W m_Z^4} \left(|g_L^{\tau\ell}|^2 + |g_R^{\tau\ell}|^2 \right) \left[1 - \frac{m_P^2}{m_\tau^2} \right]^2. \quad (40)$$

Here, the FV τ decays involve π^0 , K_s^0 , η and η' . The bounds on the decays that involve π^0 are given by $\text{Br}(\tau \rightarrow \mu\pi^0) < 1.1 \times 10^{-7}$ and $\text{Br}(\tau \rightarrow e\pi^0) < 1 \times 10^{-8}$, which translate to $\sqrt{|g_L^{\tau\mu}|^2 + |g_R^{\tau\mu}|^2} < 2.15 \times 10^{-4}$ and $\sqrt{|g_L^{\tau e}|^2 + |g_R^{\tau e}|^2} < 1.83 \times 10^{-4}$. The bounds involving K_s^0 are given by $\text{Br}(\tau \rightarrow \mu K_s^0) < 2.3 \times 10^{-8}$ and $\text{Br}(\tau \rightarrow e K_s^0) < 2.6 \times 10^{-8}$, and these translate to $\sqrt{|g_L^{\tau\mu}|^2 + |g_R^{\tau\mu}|^2} < 8.92 \times 10^{-5}$ and $\sqrt{|g_L^{\tau e}|^2 + |g_R^{\tau e}|^2} < 9.48 \times 10^{-5}$. The bounds involving η are given by $\text{Br}(\tau \rightarrow \mu\eta) < 6.5 \times 10^{-8}$ and $\text{Br}(\tau \rightarrow e\eta) < 9.8 \times 10^{-8}$, from which we obtain $\sqrt{|g_L^{\tau\mu}|^2 + |g_R^{\tau\mu}|^2} < 2.19 \times 10^{-4}$ and $\sqrt{|g_L^{\tau e}|^2 + |g_R^{\tau e}|^2} < 2.61 \times 10^{-4}$. Finally, the bounds involving η' are given by $\text{Br}(\tau \rightarrow \mu\eta') < 1.3 \times 10^{-7}$ and $\text{Br}(\tau \rightarrow e\eta') < 1.6 \times 10^{-7}$, from which we obtain $\sqrt{|g_L^{\tau\mu}|^2 + |g_R^{\tau\mu}|^2} < 4.8 \times 10^{-4}$ and $\sqrt{|g_L^{\tau e}|^2 + |g_R^{\tau e}|^2} < 5.32 \times 10^{-4}$. The Belle II experiment is expected to improve the bound on the $\tau \rightarrow \mu\eta$ decay to 10^{-9} [61], which would translate to $\sqrt{|g_L^{\tau\mu}|^2 + |g_R^{\tau\mu}|^2} < 2.72 \times 10^{-5}$.

Inspecting the bounds, we can see they are in general stronger than those obtained from meson decays by roughly one to two orders of magnitude. Thus, the FV τ decays involving mesonic final states are also a promising channel for probing FV, which highlights the potential of τ factories. We conclude this section by pointing out that the same treatment cannot be applied to the μ lepton since it is lighter than all other mesons, and thus cannot decay to a final state involving any meson.

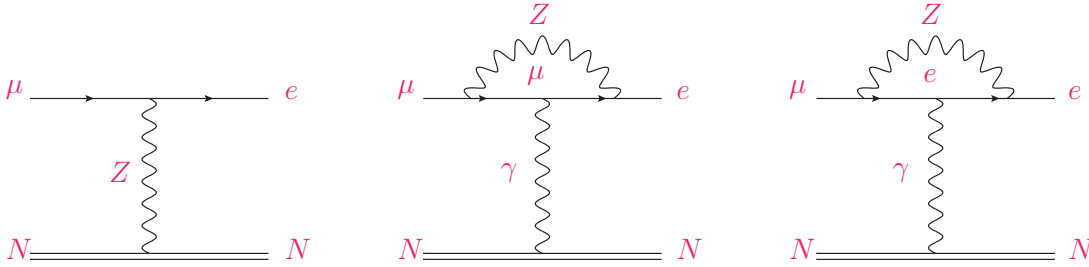


FIG. 8: Muon conversion in nuclei at tree level and at one loop.

J. μ to e Conversion in Nuclei

Very stringent constraints on the FV Z couplings to μe can be obtained from the experimental searches of muon conversion in nuclei. Such a conversion can proceed via the FV Z already at tree level as in the left diagram of Fig. 7. It can also proceed at one loop as in the remaining two diagrams in Fig. 8. Notice that in the loop diagrams, the Z loop can be integrated out to become an effective vertex by utilizing the results of $\ell_i \rightarrow \ell_j \gamma$ decay. Here we highlight the overall results and present the full details in Appendix C.

The experimental limits on the conversion rate of $\mu \rightarrow e$ in nuclei are quoted as the branching fraction of the conversion rate relative to the muon capture rate by the target nucleus. According to the SINDRUM II collaboration [60], gold yields the strongest bounds $\text{Br}^{\text{Au}}(\mu \rightarrow e) < 7 \times 10^{-13}$, which translate into the bound $\sqrt{|g_L^{\mu e}|^2 + 0.74|g_R^{\mu e}|^2} < 5.48 \times 10^{-11}$. We see that muon conversion can be quite sensitive to FV, which makes it ideal for such searches.

With regards to future experiments, the Mu2e experiment [62] is designed to use aluminum as its target material, with a projected sensitivity of $\text{Br}^{\text{Al}}(\mu \rightarrow e) < 10^{-16}$ [63]. This can yield the bound $\sqrt{|g_L^{\mu e}|^2 + 0.74|g_R^{\mu e}|^2} < 9.49 \times 10^{-13}$.

K. Muonium-antimuonium Oscillations

Muonium is a bound state of an electron and an antimuon, which can oscillate to antimuonium, a bound state of an antimuonium and a positron. In the SM, muonium-antimuonium oscillation is heavily suppressed ($\mathcal{O}(10^{-30})$), however, the transition probability can be sizable if there is a BSM contribution. The time-integrated $M \leftrightarrow \bar{M}$ oscillation is constrained by the MACS experiment at PSI to be $P(M \leftrightarrow \bar{M}) < 8.3 \times 10^{-11}$ [64]. This can be used to set bounds on the FV couplings of the Z to μe .

Muonium-antimuonium oscillation through FV Z couplings can proceed via the s - and t - channels

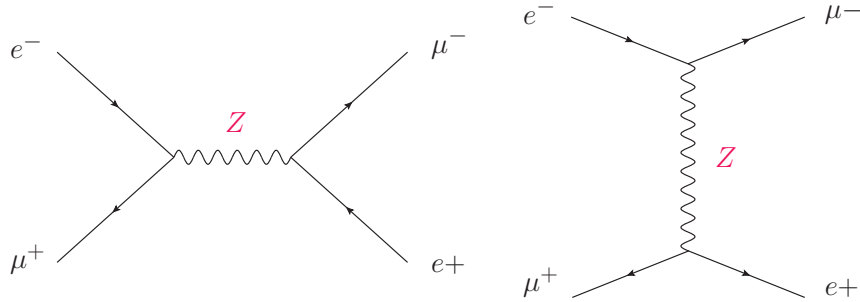


FIG. 9: Muonium-antimuonium oscillation through FV Z couplings.

as shown in Fig. 9. The details of how to calculate the time-integrated transition probability is provided in Appendix D, with the transition probability provided in Eq. (D3). Thus, the bound is obtained by requiring that $P_{\text{Th}} < P_{\text{MACS}}$. Given that the MACS experiment used a magnetic field of strength $B = 0.1$ Tesla, we obtain the bound

$$(|g_L^{\mu e}|^2 + |g_R^{\mu e}|^2)^2 + 6.5|g_L^{\mu e}|^2|g_R^{\mu e}|^2 - 2.32(|g_L^{\mu e}|^2 + |g_R^{\mu e}|^2)\text{Re}(g_L^{\mu e}g_R^{\mu e*}) < 2.72 \times 10^{-6}. \quad (41)$$

L. The $g - 2$ Anomaly

Theoretically, it is possible for FV Z couplings to solve the $g - 2$ anomaly via a FV Z loop correction to the $\gamma\mu\mu$ vertex, however, given that the size of the couplings needed to solve the anomaly is $g \gtrsim \mathcal{O}(10^{-3})$ as suggested by the proposed solution with a Z' , we can see that the above bounds exclude this possibility.

We conclude this section by summarizing all the bounds and projections in Fig. 10.

IV. CONCLUSIONS AND OUTLOOK

In this paper, we studied and set upper bounds on the FV couplings of the Z boson to charged leptons. Specifically, we have studied the bounds from direct searches from the LHC, LEP $e^+e^- \rightarrow \mu^+\mu^-, \tau^+\tau^-$ searches, FV loop corrections to flavor-conserving Z decays to leptons, corrections to EWPO, $l_i \rightarrow l_j\gamma$ decays, $l_i \rightarrow 3l_j$ decays, $l_i \rightarrow l_j + \text{inv.}$ decays, FV leptonic meson decays, $\tau \rightarrow \mu(e) + \text{meson}$ decays, muon conversion in nuclei and from muonium-antimuonium oscillation.

For Z couplings to $\tau\mu$, we found that $\tau \rightarrow \mu\gamma$ yielded the strongest bounds, at a level of $\mathcal{O}(10^{-5})$, followed by $\tau \rightarrow 3\mu$. We also found that future experiments could improve the bound to $\mathcal{O}(10^{-6})$. On the other hand, for Z couplings to τe , we found that $\tau \rightarrow 3e, \mu\mu e$ yielded the strongest bounds,

as several of the processes discussed here are novel, such as the decays involving mesons, it would be interesting to evaluate the bounds that can be extracted from them on the Higgs interactions. We plan to do this in a future work. We conclude by pointing out that FV represents an interesting venue for potential BSM physics and thus merits attention.

Acknowledgment

We thank Sacha Davidson for the valuable discussion. A.A. is funded by the University of Sharjah under the research projects No 21021430107 “*Hunting for New Physics at Colliders*” and No 23021430135 “*Terascale Physics: Colliders vs Cosmology*”. The work of NO is supported in part by the United States Department of Energy Grant, Nos. DE-SC0012447 and DC-SC0023713.

Appendix A: Detailed Calculation of the $\ell_i \rightarrow \ell_j \gamma$ Decay

Here, we provide the detailed derivation of the decay width of $\ell_i \rightarrow \ell_j \gamma$. In our calculation, we will drop all terms $\sim O(m_{i,j}/m_Z)$. At this level of approximation, the leg corrections where the photon is radiated from outside the loop are subleading and can be dropped. The matrix element of the Feynman diagrams shown in Fig. 5 are given by

$$\begin{aligned} \mathcal{M} = e\bar{u}(q_2) & \left[(g_L^{ij*} P_R + g_R^{ij*} P_L) I(p, q_1, m_i) (g_L P_L + g_R P_R) \right. \\ & \left. + (g_L P_R + g_R P_L) I(p, q_1, m_j) (g_L^{ij*} P_L + g_R^{ij*} P_R) \right] u(p) \epsilon_\nu^*(q_1), \end{aligned} \quad (\text{A1})$$

where the loop integral is given by

$$I(p, q_1, m) = \int \frac{d^4 k}{(2\pi)^4} \frac{\gamma^\beta (\not{p} - \not{k} - \not{q}_1 + m) \gamma^\nu (\not{p} - \not{k} + m) \gamma^\alpha (g_{\alpha\beta} - k_\alpha k_\beta / m_Z^2)}{[(p - k - q_1)^2 - m^2][(p - k)^2 - m^2][k^2 - m_Z^2]}. \quad (\text{A2})$$

Evaluating the integral using dimensional regularization in the \overline{MS} scheme, and dropping m_j since $m_\tau \gg m_\mu \gg m_e$, we obtain

$$\mathcal{M} \simeq \frac{3ie}{32\pi^2} \bar{u}(q_2) \gamma^\mu \left[(g_L^{ij*} P_L + g_R^{ij*} P_R) (g_L P_L + g_R P_R) + (g_L P_L + g_R P_R) (g_L^{ij*} P_L + g_R^{ij*} P_R) \right] u(p) \epsilon_\mu^*(q_1), \quad (\text{A3})$$

and upon integrating $|\mathcal{M}|^2$ over the phase space, we obtain Eq. 30.

Appendix B: Detailed Calculation of $\ell_i \rightarrow \ell_j + \ell_k + \bar{\ell}_k$

There are two contributions to this process as shown in Fig. 6. The amplitude of the Z -mediated diagram can be written as

$$\mathcal{M}_1 = \frac{-i(g_{\mu\nu} - \frac{(k_2+k_3)_\mu(k_2+k_3)_\nu}{m_Z^2})}{(k_2+k_3)^2 - m_Z^2} \bar{u}(k_2)\gamma^\nu(g_L P_L + g_R P_R)v(k_3)\bar{u}(k_1)\gamma^\mu(g_L^{ij*} P_L + g_R^{ij*} P_R)u(p). \quad (\text{B1})$$

On the other hand, one can use the results in Eq. (A3) to integrate out the loop and write the interaction as an effective vertex. With this, the amplitude of the second diagram reads

$$\begin{aligned} \mathcal{M}_2 = & \frac{3ie^2}{32\pi^2} \frac{1}{(p-k_1)^2} \bar{u}(k_2)\gamma^\mu v(k_3)\bar{u}(k_1)\gamma_\mu \\ & \times \left[(g_L^{ij*} P_L + g_R^{ij*} P_R)(g_L P_L + g_R P_R) + (g_L P_L + g_R P_R)(g_L^{ij*} P_L + g_R^{ij*} P_R) \right] u(p), \quad (\text{B2}) \end{aligned}$$

and the total matrix element is given by $\mathcal{M} = \mathcal{M}_1 + \mathcal{M}_2$. In general, the integrals are complex and the result is not very illuminating, however, as it turns out, the second diagram dominates by orders of magnitude compared to the first. Thus, we can drop \mathcal{M}_1 . In addition, we can treat the final state as massless since this only amounts to dropping terms $\mathcal{O}(m_i/m_z)$. Thus, upon integrating $|\mathcal{M}_2|^2$ over the phase space, we obtain Eq. 31. We have verified numerically that our approximations are justified.

Appendix C: Detailed Calculation of the Muon Conversion in Nuclei

Following the convention of [59], we can write the most general effective Lagrangian for muon conversion in nuclei as follows

$$\begin{aligned} \mathcal{L} = & c_L \frac{em_\mu}{8\pi^2} (\bar{e}\sigma^{\alpha\beta} P_L \mu) F_{\alpha\beta} - \frac{1}{2} \sum_q \left[g_{LS}^q (\bar{e} P_R \mu) (\bar{q} q) + g_{LP}^q (\bar{e} P_R \mu) (\bar{q} \gamma_5 q) + g_{LV}^q (\bar{e} \gamma^\alpha P_L \mu) \right. \\ & \left. \times (\bar{q} \gamma_\alpha q) + g_{LA}^q (\bar{e} \gamma^\alpha P_L \mu) (\bar{q} \gamma_\alpha \gamma_5 q) + \frac{1}{2} g_{LT}^q (\bar{e} \sigma^{\alpha\beta} P_R \mu) (\bar{q} \sigma_{\alpha\beta} q) + (L \leftrightarrow R) \right], \quad (\text{C1}) \end{aligned}$$

where the first term arises from the magnetic dipole operator after integrating out the loop, the first term inside the square brackets is the scalar operator, the second is the pseudoscalar operator, the third and fourth are the vector and axial vector operators respectively, and the last one is the tensor operator. Inspecting the Feynman diagrams in Fig. 8, we can see that we don't have any diagrams contributing to the scalar, pseudoscalar, or tensor operators. Thus we have $g_{LS}^q = g_{RS}^q = g_{LP}^q = g_{RP}^q = g_{LT}^q = g_{RT}^q = 0$. On the other hand, the first diagram contributes to $g_{LV}^q, g_{RV}^q, g_{LA}^q$

and g_{LA}^q , whereas the second and the third diagrams contribute to all three remaining operators. Now, to extract coefficients $c_{L,R}$, we can use the magnetic dipole operator to write the effective vertex after integrating out the loops in the second and third diagrams in Fig. 8 as follows

$$\mathcal{M} = \frac{em_\mu}{4\pi^2} \bar{u}(q_2) \left[c_L \not{q}_1 \gamma^\nu P_L + c_R \not{q}_1 \gamma^\nu P_R + c_L^* P_R \gamma^\nu \not{q}_1 + c_R^* P_L \gamma^\nu \not{q}_1 \right] u(p) \epsilon^*(q_1), \quad (\text{C2})$$

which is to be matched to the exact result found in Eq. (A3). A simple calculation yields the matching

$$c_L = -\frac{3}{8m_\mu^2} g_R g_R^{\mu e*}, \quad (\text{C3})$$

$$c_R = -\frac{3}{8m_\mu^2} g_L g_L^{\mu e*}. \quad (\text{C4})$$

Turning our attention to extracting the vector and axial coefficients, first notice that the matrix element of the first diagram is given by

$$\mathcal{M}_1 = \bar{u}(k_1) \gamma^\alpha (g_L^{\mu e*} P_L + g_R^{\mu e*} P_R) u(p_1) \frac{\left[g_{\alpha\beta} - \frac{1}{m_Z^2} (p_1 - k_1)_\alpha (p_1 - k_1)_\beta \right]}{(p_1 - k_1)^2 - m_Z^2} \bar{u}(k_2) \gamma^\beta (g_V^q - g_A^q \gamma_5) u(p_2), \quad (\text{C5})$$

where g_V^q and g_A^q are the vector and axial couplings of the Z to quarks. In the non-relativistic limit, we can assume that $E_\mu \ll m_\mu$, $E_N \ll m_N$ and that the momentum transfer to the nucleus is negligible, in which case, Eq. (C5) can be approximated as

$$\mathcal{M}_1 = -\frac{1}{M_Z^2} \times \bar{u}(k_1) \gamma^\alpha (g_L^{\mu e*} P_L + g_R^{\mu e*} P_R) u(p_1) \bar{u}(k_2) \gamma_\alpha (g_V^q - g_A^q \gamma_5) u(p_2). \quad (\text{C6})$$

On the other hand, the contribution of the second and third diagrams of Fig. (8) can be obtained using Eq. (A3), which after some simplification reads

$$\mathcal{M}_2 \simeq -\frac{3e^2}{32\pi^2} \frac{1}{(p_1 - k_1)^2} \bar{u}(k_1) \gamma^\alpha (g_L g_L^{\mu e*} P_L + g_R g_R^{\mu e*} P_R) u(p_1) \bar{u}(k_2) \gamma_\alpha u(p_2), \quad (\text{C7})$$

and the total contribution is given by $\mathcal{M} = \mathcal{M}_1 + \mathcal{M}_2$. Now, it's easy to extract the vector and axial coefficients, which are found to be

$$\begin{aligned} g_{LV}^q &\simeq \left(\frac{2}{m_Z^2} g_V^q + \frac{3\alpha}{4\pi m_\mu^2} g_L \right) g_L^{\mu e*}, \\ g_{RV}^q &\simeq \left(\frac{2}{m_Z^2} g_V^q + \frac{3\alpha}{4\pi m_\mu^2} g_R \right) g_R^{\mu e*}, \\ g_{LA}^q &= -\frac{2}{m_Z^2} g_A^q g_L^{\mu e*}, \\ g_{RA}^q &= -\frac{2}{m_Z^2} g_A^q g_R^{\mu e*}. \end{aligned} \quad (\text{C8})$$

Now that we have all the EFT coefficients, we can proceed with calculating the $\mu \rightarrow e$ conversion rate. Following [59], the matrix elements that contribute to the conversion are $\langle N | \bar{q}q | N \rangle$, $\langle N | \bar{q}\gamma^\mu q | N \rangle$ and $\langle N | \bar{q}F^{\mu\nu} q | N \rangle$, whereas $\langle N | \bar{q}\gamma^\mu \gamma_5 q | N \rangle$ vanishes. This implies that we can neglect $g_{LR,A}^q$. Therefore, we can express the conversion rate as

$$\Gamma(\mu \rightarrow e) = \left| -\frac{e}{16\pi^2} c_R D + \tilde{g}_{LV}^{(p)} V^{(p)} + \tilde{g}_{LV}^{(n)} V^{(n)} \right|^2 + \left| -\frac{e}{16\pi^2} c_L D + \tilde{g}_{RV}^{(p)} V^{(p)} + \tilde{g}_{RV}^{(n)} V^{(n)} \right|^2, \quad (\text{C9})$$

where

$$\begin{aligned} \tilde{g}_{LV,RV}^{(p)} &= 2g_{LV,RV}^{(u)} + g_{LV,RV}^{(d)}, \\ \tilde{g}_{LV,RV}^{(n)} &= g_{LV,RV}^{(u)} + 2g_{LV,RV}^{(d)}, \end{aligned} \quad (\text{C10})$$

and the coefficients D , $V^{(p)}$ and $V^{(n)}$ are the overlap integrals between the muon, electron and nucleus wavefunctions, which can be found for various target materials in [59]. Notice that for neutrons, the second term of $g_{LV,RV}^{(n)}$ vanishes due to the lack of an electric charge. According to the SINDRUM II collaboration [60], gold yields the strongest bound on the conversion rate

$$\text{Br}^{\text{Au}}(\mu \rightarrow e) = \left[\frac{\Gamma(\mu \rightarrow e)}{\Gamma_{\text{Capture}}(\mu)} \right]_{\text{Au}} < 7 \times 10^{-13} \quad @ 90\% \text{ CL}, \quad (\text{C11})$$

where the muon capture rate in gold is given by $\Gamma_{\text{Capture}}^{\text{Au}} = 13.07 \times 10^6 \text{ s}^{-1}$, and the overlap integrals for gold are given by $V_{\text{Au}}^{(p)} = 0.0974 m_\mu^{5/2}$, $V_{\text{Au}}^{(n)} = 0.146 m_\mu^{5/2}$, and $D_{\text{Au}} = 0.189 m_\mu^{5/2}$. On the other hand, the MU2e experiment [62] is designed to use aluminum as a target material, and is projected to have a sensitivity of [63]

$$\text{Br}^{\text{Al}}(\mu \rightarrow e) = \left[\frac{\Gamma(\mu \rightarrow e)}{\Gamma_{\text{Capture}}(\mu)} \right]_{\text{Al}} < 10^{-16} \quad @ 90\% \text{ CL}, \quad (\text{C12})$$

and for aluminum, the muon capture rate is given by $\Gamma_{\text{Capture}}^{\text{Al}} = 0.7054 \times 10^6 \text{ s}^{-1}$, and the overlap integrals for aluminum are given by $V_{\text{Al}}^{(p)} = 0.0161 m_\mu^{5/2}$, $V_{\text{Al}}^{(n)} = 0.0173 m_\mu^{5/2}$, and $D_{\text{Al}} = 0.0362 m_\mu^{5/2}$.

Appendix D: Detailed Calculation of $M \leftrightarrow \bar{M}$ Oscillation

We can write the interaction Lagrangian of the muonium-antimuonium oscillation as follows [65] (see also [66])

$$\mathcal{L}_{M \leftrightarrow \bar{M}} = - \sum_{i=1}^5 \frac{G_i}{\sqrt{2}} Q_i, \quad (\text{D1})$$

where Q_i are all the possible operators that can induce $M \leftrightarrow \bar{M}$ oscillation, which are given by

$$\begin{aligned}
Q_1 &= [\bar{\mu}\gamma_\alpha(1 - \gamma_5)e][\bar{\mu}\gamma^\alpha(1 - \gamma_5)e], \\
Q_2 &= [\bar{\mu}\gamma_\alpha(1 + \gamma_5)e][\bar{\mu}\gamma^\alpha(1 + \gamma_5)e], \\
Q_3 &= [\bar{\mu}\gamma_\alpha(1 + \gamma_5)e][\bar{\mu}\gamma^\alpha(1 - \gamma_5)e], \\
Q_4 &= [\bar{\mu}(1 - \gamma_5)e][\bar{\mu}(1 - \gamma_5)e], \\
Q_5 &= [\bar{\mu}(1 + \gamma_5)e][\bar{\mu}(1 + \gamma_5)e],
\end{aligned} \tag{D2}$$

with all other operators related to the 5 above by linear combination and Fierz identities. Inspecting the Feynman diagrams in Fig. 9, it is quite obvious that only Q_1 , Q_2 and Q_3 contribute to the oscillation. In [66], the time-integrated transition probability was calculated, however, they did not take into account the magnetic dependence, which was treated in [67]. The treatment of [67] was applied in [68] to the Z' , so we use their results. The theoretical time-integrated transition probability was found to be

$$\begin{aligned}
P_{\text{Th}} &= \frac{64}{\pi^2} m_{\text{red}}^6 \alpha^6 \tau^2 G_F^2 \left[|C_{0,0}|^2 \left| -G_3 + \frac{G_1 + G_2 - \frac{1}{2}G_3}{\sqrt{1 + X^2}} \right|^2 + |C_{1,0}|^2 \left| G_3 + \frac{G_1 + G_2 - \frac{1}{2}G_3}{\sqrt{1 + X^2}} \right|^2 \right], \\
&= \frac{2.57 \times 10^{-5}}{G_F^2} \left[|C_{0,0}|^2 \left| -G_3 + \frac{G_1 + G_2 - \frac{1}{2}G_3}{\sqrt{1 + X^2}} \right|^2 + |C_{1,0}|^2 \left| G_3 + \frac{G_1 + G_2 - \frac{1}{2}G_3}{\sqrt{1 + X^2}} \right|^2 \right], \tag{D3}
\end{aligned}$$

where G_F is the Fermi constant, $\tau = 2.2\mu\text{s}$ is the lifetime of the muon, $m_{\text{red}} = m_\mu m_e / (m_\mu + m_e) \simeq m_e$ is the reduced mass of the muonium, X encodes the magnetic flux density, which is given by $X \simeq 6.31B/\text{Tesla}$ (see the Appendix B of [68] for the more detail), and $|C_{F,m}|^2$ denote the population of the muonium states with a total angular momentum = F and an angular momentum in the \hat{z} direction = m . In our calculation, we use the same values quotes in [67], which are $|C_{0,0}|^2 = 0.32$ and $|C_{1,0}|^2 = 0.18$.

Now, the coefficients G_i are model-dependent, and have been found for Z' in [68]. Thus, we can easily extend their results to the case of a FV Z . We find

$$\begin{aligned}
G_1 &= \frac{\sqrt{2}|g_L^{\mu e}|^2}{8m_Z^2}, \\
G_2 &= \frac{\sqrt{2}|g_R^{\mu e}|^2}{8m_Z^2}, \\
G_3 &= \frac{2\sqrt{2}g_L^{\mu e}g_R^{\mu e*}}{8m_Z^2}.
\end{aligned} \tag{D4}$$

[1] G. Aad *et al.* [ATLAS], ‘‘Observation of a new particle in the search for the Standard Model Higgs boson with the ATLAS detector at the LHC,’’ Phys. Lett. B **716** (2012), 1-29; [hep-ex/1207.7214](#). S. Cha-

- trchyan *et al.* [CMS], “Observation of a New Boson at a Mass of 125 GeV with the CMS Experiment at the LHC,” *Phys. Lett. B* **716** (2012), 30-61 [hep-ex/1207.7235](#). I
- [2] S. Chang and M. A. Luty, “The Higgs Trilinear Coupling and the Scale of New Physics,” *JHEP* **03** (2020), 140 [hep-ph/1902.05556](#). I
- [3] F. Abu-Ajamieh, S. Chang, M. Chen and M. A. Luty, “Higgs coupling measurements and the scale of new physics,” *JHEP* **07**, 056 (2021) [hep-ph/2009.11293](#).
- [4] F. Abu-Ajamieh, “The scale of new physics from the Higgs couplings to $\gamma\gamma$ and γZ ,” *JHEP* **06**, 091 (2022) [hep-ph/2112.13529](#).
- [5] F. Abu-Ajamieh, “The scale of new physics from the Higgs couplings to gg ,” *Phys. Lett. B* **833**, 137389 (2022) [hep-ph/2203.07410](#). I
- [6] S. L. Glashow, J. Iliopoulos and L. Maiani, *Phys. Rev. D* **2** (1970), 1285-1292 I
- [7] J. D. Bjorken and S. Weinberg, “A Mechanism for Nonconservation of Muon Number,” *Phys. Rev. Lett.* **38**, 622 (1977) I
- [8] B. McWilliams and L. F. Li, *Nucl. Phys. B* **179**, 62-84 (1981)
- [9] O. U. Shanker, “Flavor Violation, Scalar Particles and Leptoquarks,” *Nucl. Phys. B* **206**, 253-272 (1982)
- [10] S. M. Barr and A. Zee, “Electric Dipole Moment of the Electron and of the Neutron,” *Phys. Rev. Lett.* **65**, 21-24 (1990) [erratum: *Phys. Rev. Lett.* **65**, 2920 (1990)]
- [11] K. S. Babu and S. Nandi, “Natural fermion mass hierarchy and new signals for the Higgs boson,” *Phys. Rev. D* **62**, 033002 (2000) [hep-ph/hep-ph/9907213](#).
- [12] J. L. Diaz-Cruz and J. J. Toscano, “Lepton flavor violating decays of Higgs bosons beyond the standard model,” *Phys. Rev. D* **62**, 116005 (2000) [hep-ph/hep-ph/9910233](#).
- [13] T. Han and D. Marfatia, “ $h \rightarrow \mu \tau$ at hadron colliders,” *Phys. Rev. Lett.* **86**, 1442-1445 (2001) [hep-ph/hep-ph/0008141](#).
- [14] M. Blanke, A. J. Buras, B. Duling, S. Gori and A. Weiler, “ $\Delta F=2$ Observables and Fine-Tuning in a Warped Extra Dimension with Custodial Protection,” *JHEP* **03**, 001 (2009) [hep-ph/0809.1073](#).
- [15] S. Casagrande, F. Goertz, U. Haisch, M. Neubert and T. Pfoh, “Flavor Physics in the Randall-Sundrum Model: I. Theoretical Setup and Electroweak Precision Tests,” *JHEP* **10**, 094 (2008) [hep-ph/0807.4937](#).
- [16] G. F. Giudice and O. Lebedev, “Higgs-dependent Yukawa couplings,” *Phys. Lett. B* **665**, 79-85 (2008) [hep-ph/0804.1753](#).
- [17] J. A. Aguilar-Saavedra, “A Minimal set of top-Higgs anomalous couplings,” *Nucl. Phys. B* **821**, 215-227 (2009) [hep-ph/0904.2387](#).
- [18] M. E. Albrecht, M. Blanke, A. J. Buras, B. Duling and K. Gemmler, “Electroweak and Flavour Structure of a Warped Extra Dimension with Custodial Protection,” *JHEP* **09**, 064 (2009) [hep-ph/0903.2415](#).
- [19] A. J. Buras, B. Duling and S. Gori, “The Impact of Kaluza-Klein Fermions on Standard Model Fermion Couplings in a RS Model with Custodial Protection,” *JHEP* **09**, 076 (2009) [hep-ph/0905.2318](#).
- [20] K. Agashe and R. Contino, “Composite Higgs-Mediated FCNC,” *Phys. Rev. D* **80**, 075016 (2009)

- hep-ph/0906.1542.
- [21] A. Goudelis, O. Lebedev and J. h. Park, “Higgs-induced lepton flavor violation,” *Phys. Lett. B* **707**, 369-374 (2012) hep-ph/1111.1715.
- [22] A. Arhrib, Y. Cheng and O. C. W. Kong, “Higgs to $\mu^+\tau$ Decay in Supersymmetry without R-parity,” *EPL* **101**, no.3, 31003 (2013) hep-ph/1208.4669.
- [23] D. McKeen, M. Pospelov and A. Ritz, “Modified Higgs branching ratios versus CP and lepton flavor violation,” *Phys. Rev. D* **86**, 113004 (2012) hep-ph/1208.4597.
- [24] A. Azatov, M. Toharia and L. Zhu, “Higgs Mediated FCNC’s in Warped Extra Dimensions,” *Phys. Rev. D* **80**, 035016 (2009) hep-ph/0906.1990.
- [25] G. Blankenburg, J. Ellis and G. Isidori, “Flavour-Changing Decays of a 125 GeV Higgs-like Particle,” *Phys. Lett. B* **712**, 386-390 (2012) hep-ph/1202.5704.
- [26] S. Kanemura, T. Ota and K. Tsumura, “Lepton flavor violation in Higgs boson decays under the rare tau decay results,” *Phys. Rev. D* **73**, 016006 (2006) hep-ph/hep-ph/0505191.
- [27] S. Davidson and G. J. Grenier, “Lepton flavour violating Higgs and tau to mu gamma,” *Phys. Rev. D* **81**, 095016 (2010) hep-ph/1001.0434.
- [28] R. Harnik, J. Kopp and J. Zupan, “Flavor Violating Higgs Decays,” *JHEP* **03**, 026 (2013) hep-ph/1209.1397. IV
- [29] F. Abu-Ajamieh and S. K. Vempati, “Can the Higgs still account for the $g-2$ anomaly?,” *Int. J. Mod. Phys. A* **38**, no.20, 2350091 (2023) hep-ph/2209.10898.
- [30] F. Abu-Ajamieh, M. Frasca and S. K. Vempati, “Flavor Violating Di- Higgs Coupling,” hep-ph/2305.17362. I
- [31] G. D’Ambrosio, G. F. Giudice, G. Isidori and A. Strumia, “Minimal flavor violation: An Effective field theory approach,” *Nucl. Phys. B* **645**, 155-187 (2002) hep-ph/hep-ph/0207036. I
- [32] A. Brignole and A. Rossi, “Anatomy and phenomenology of mu-tau lepton flavor violation in the MSSM,” *Nucl. Phys. B* **701**, 3-53 (2004) hep-ph/hep-ph/0404211. I
- [33] S. Davidson, S. Lacroix and P. Verdier, “LHC sensitivity to lepton flavour violating Z boson decays,” *JHEP* **09**, 092 (2012) hep-ph/1207.4894. II
- [34] T. Goto, R. Kitano and S. Mori, “Lepton flavor violating Z-boson couplings from nonstandard Higgs interactions,” *Phys. Rev. D* **92**, 075021 (2015) hep-ph/1507.03234.
- [35] J. F. Kamenik, A. Korajac, M. Szewc, M. Tammaro and J. Zupan, “Flavor-violating Higgs and Z boson decays at a future circular lepton collider,” *Phys. Rev. D* **109**, no.1, L011301 (2024) hep-ph/2306.17520.
- [36] A. Jueid, J. Kim, S. Lee, J. Song and D. Wang, “Exploring lepton flavor violation phenomena of the Z and Higgs bosons at electron-proton colliders,” *Phys. Rev. D* **108**, no.5, 055024 (2023) hep-ph/2305.05386. I
- [37] R. S. Chivukula and E. H. Simmons, “Electroweak limits on nonuniversal Z-prime bosons,” *Phys. Rev. D* **66**, 015006 (2002) hep-ph/hep-ph/0205064. I

- [38] J. Erler, P. Langacker, S. Munir and E. Rojas, “Improved Constraints on Z-prime Bosons from Electroweak Precision Data,” JHEP **08**, 017 (2009) [hep-ph/0906.2435](#).
- [39] J. I. Aranda, F. Ramirez-Zavaleta, J. J. Toscano and E. S. Tututi, “Bounding the $Z'tc$ coupling from $D^0 - \bar{D}^0$ mixing and single top production at the ILC,” J. Phys. G **38**, 045006 (2011) [hep-ph/1007.3326](#).
- [40] B. Murakami, “The Impact of lepton flavor violating Z-prime bosons on muon g-2 and other muon observables,” Phys. Rev. D **65**, 055003 (2002) [hep-ph/hep-ph/0110095](#).
- [41] W. Altmannshofer, C. Y. Chen, P. S. Bhupal Dev and A. Soni, Phys. Lett. B **762**, 389-398 (2016) [hep-ph/1607.06832](#). I
- [42] W. Buchmuller and D. Wyler, “Effective Lagrangian Analysis of New Interactions and Flavor Conservation,” Nucl. Phys. B **268**, 621-653 (1986) II
- [43] B. Grzadkowski, M. Iskrzynski, M. Misiak and J. Rosiek, “Dimension-Six Terms in the Standard Model Lagrangian,” JHEP **10**, 085 (2010) [hep-ph/1008.4884](#).II
- [44] S. Dawson and A. Ismail, “Standard model EFT corrections to Z boson decays,” Phys. Rev. D **98**, no.9, 093003 (2018) [hep-ph/1808.05948](#). II
- [45] E. E. Jenkins, A. V. Manohar and P. Stoffer, “Low-Energy Effective Field Theory below the Electroweak Scale: Operators and Matching,” JHEP **03**, 016 (2018) [erratum: JHEP **12**, 043 (2023)] [hep-ph/1709.04486](#). II
- [46] G. Aad *et al.* [ATLAS], “Search for the charged-lepton-flavor-violating decay $Z \rightarrow e\mu$ in pp collisions at $\sqrt{s} = 13$ TeV with the ATLAS detector,” Phys. Rev. D **108**, 032015 (2023) [hep-ex/2204.10783](#). III A
- [47] G. Aad *et al.* [ATLAS], “Search for lepton-flavor-violation in Z-boson decays with τ -leptons with the ATLAS detector,” Phys. Rev. Lett. **127**, 271801 (2022) [hep-ex/2105.12491](#). III A
- [48] J. Alcaraz *et al.* [ALEPH, DELPHI, L3, OPAL and LEP Electroweak Working Group], “A Combination of preliminary electroweak measurements and constraints on the standard model,” [hep-ex/hep-ex/0612034](#). III B
- [49] J. Haller, A. Hoecker, R. Kogler, K. Moenig, T. Peiffer and J. Stelzer, “Update of the global electroweak fit and constraints on two-Higgs-doublet models,” Eur. Phys. J. C **78** (2018) no.8, 675 [hep-ph/1803.01853](#). III D
- [50] P.A. Zyla *et al.* (Particle Data Group), Prog. Theor. Exp. Phys. 2020, 083C01 (2020) III C, III D, III F, III F, III G, III G, III G, III G, III H, III H, III H, III H, III I
- [51] R. Bayes *et al.* [TWIST], “Search for two body muon decay signals,” Phys. Rev. D **91**, no.5, 052020 (2015) [hep-ex/1409.0638](#). III E
- [52] N. Tsuzuki *et al.* [Belle], “Search for lepton-flavor-violating τ decays into a lepton and a vector meson using the full Belle data sample,” JHEP **06**, 118 (2023) [hep-ex/2301.03768](#). III E
- [53] I. Adachi *et al.* [Belle-II], “Search for Lepton-Flavor-Violating τ Decays to a Lepton and an Invisible Boson at Belle II,” Phys. Rev. Lett. **130**, no.18, 181803 (2023) [hep-ex/2212.03634](#). III E
- [54] A. K. Perrevoort [Mu3e], “The Rare and Forbidden: Testing Physics Beyond the Standard Model with

- Mu3e,” SciPost Phys. Proc. **1**, 052 (2019) [hep-ex/1812.00741](#).
- [55] L. Calibbi and G. Signorelli, “Charged Lepton Flavour Violation: An Experimental and Theoretical Introduction,” Riv. Nuovo Cim. **41**, no.2, 71-174 (2018) [hep-ph/1709.00294](#).
- [56] D. E. Hazard, “Lepton flavor violating meson decays,” [hep-ph/1710.00117](#). III H
- [57] D. Delepine, M. Napsuciale and E. Peinado, “Effects of an H-mu-tau coupling in quarkonium lepton flavor violation decays,” [hep-ph/1509.04057](#). III H
- [58] <https://halldweb.jlab.org/DocDB/0033/003345/002/dalitz.pdf>
- [59] R. Kitano, M. Koike and Y. Okada, “Detailed calculation of lepton flavor violating muon electron conversion rate for various nuclei,” Phys. Rev. D **66**, 096002 (2002) [erratum: Phys. Rev. D **76**, 059902 (2007)] [hep-ph/hep-ph/0203110](#). C, C, C
- [60] W. H. Bertl *et al.* [SINDRUM II], “A Search for muon to electron conversion in muonic gold,” Eur. Phys. J. C **47**, 337-346 (2006) III J, C
- [61] T. Abe *et al.* [Belle-II], “Belle II Technical Design Report,” [physics.ins-det/1011.0352](#). III I
- [62] L. Bartoszek *et al.* [Mu2e], “Mu2e Technical Design Report,” [physics.ins-det/1501.05241](#). III J, C
- [63] M. Kargiantoulakis, “A Search for Charged Lepton Flavor Violation in the Mu2e Experiment,” Mod. Phys. Lett. A **35**, no.19, 2030007 (2020) [hep-ex/2003.12678](#). III J, C
- [64] L. Willmann, P. V. Schmidt, H. P. Wirtz, R. Abela, V. Baranov, J. Bagaturia, W. H. Bertl, R. Engfer, A. Grossmann and V. W. Hughes, *et al.* “New bounds from searching for muonium to anti-muonium conversion,” Phys. Rev. Lett. **82**, 49-52 (1999) [hep-ex/hep-ex/9807011](#). III K
- [65] R. Conlin and A. A. Petrov, “Muonium-antimuonium oscillations in effective field theory,” Phys. Rev. D **102**, no.9, 095001 (2020) [hep-ph/2005.10276](#). D
- [66] T. E. Clark and S. T. Love, “Muonium - anti-muonium oscillations and massive Majorana neutrinos,” Mod. Phys. Lett. A **19**, 297-306 (2004) [hep-ph/hep-ph/0307264](#). D, D
- [67] T. Fukuyama, Y. Mimura and Y. Uesaka, “Models of the muonium to antimuonium transition,” Phys. Rev. D **105**, no.1, 015026 (2022) [hep-ph/2108.10736](#). D, D
- [68] J. Kriewald, J. Orloff, E. Pinsard and A. M. Teixeira, “Prospects for a flavour violating Z' explanation of $\Delta a_{\mu,e}$,” Eur. Phys. J. C **82**, no.9, 844 (2022) [hep-ph/2204.13134](#).
- D, D